# Analysis of Punch-Through Breakdown Voltages in 3C-SiC Schottky Barrier Diode using Gaussian profile for 200µm thick wafers

Thesis submitted towards the partial fulfilment of requirement for the award of the degree of

**Master of Engineering**

**In**

**Electronics and Communication Engineering**


**Submitted by:**

Pratibha Nishad

Roll No.: 801261015

**Under the guidance of:**

Dr. A. K. Chatterjee

Professor, ECED



**ELECTRONICS AND COMMUNICATION ENGINEERING DEPARTMENT**

**THAPAR UNIVERSITY**

**(Established under the section 3 of UGC Act, 1956)**

**PATIALA – 147004 (PUNJAB)**


**JULY 2014**

## CERTIFICATE

I hereby certify that the thesis entitled **"Analysis of Punch Through Breakdown Voltages in 3C-SiC Schottky Barrier Diode using Gaussian profile for 200µm thick wafers"** is an authentic record of my work carried out as requirement for the award of degree of Master of Engineering (Electronics and Communication Engineering) at Thapar University, Patiala, under the supervision of Dr. A. K. Chatterjee, Professor, Electronics and Communication Engineering Department, Thapar University, Patiala.

Date: 2-06-2014

Pratibha Nishad

(801261015)

It is certified that the above statement made by the student is correct to the best of my knowledge and belief.

Date: 2.6.14

Dr. A. K. Chatterjee

Professor

ECED

Dr. Sanjay Sharma

Professor and Head

ECED, Thapar University,

Patiala(Punjab)-147004

Dr. S.K. Mohapatra

Dean, Academic Affairs

Thapar University,

Patiala(Punjab)-147004

# ACKNOWLEDGEMENT

I would like to express my gratitude to Dr. A. K. Chatterjee, Professor, Electronics and Communication Engineering Department, Thapar University, Patiala for his patience guidance and support throughout this report work. I am truly very fortunate to have the opportunity to work with him. He has provided help in technical writing, presentation style and I found this guidance to be extremely valuable.

I am also thankful to entire faculty, staff members and H.O.D of Electronics & Communication Engineering Department for their encouragement.

I am greatly indebted to all my friends, who have graciously applied themselves to the task of helping me with ample moral support and valuable suggestion. Finally, I would like to extend my gratitude to all those persons who directly or indirectly helped me in process and contributed toward this work.

**Pratibha Nishad**

**801261015**

# ABSTRACT

Normally Schottky Barrier diodes are designed by using a uniform doping profile of the semiconductor material used. However, the higher breakdown voltage can be achieved by using non-uniform doping profiles, namely, linearly graded profile, Gaussian profile and Complementary error function profile.

The present work aims at analyzing the punch through breakdown voltage of 3C-SiC Schottky Barrier diode using Gaussian profile. It is seen that Schottky barrier diode yield high punch through breakdown voltage with higher values of peak doping level and lower values of constant m. So, it is possible to design Schottky barrier diode with thinner wafers of 3C-SiC and higher breakdown voltage using Gaussian profile.

# Table of Contents

# List of Figures

# List of Tables

# CHAPTER 1

# INTRODUCTION

## 1.1 Silicon Carbide

Silicon Carbide(SiC) is a wide band gap semiconductor that has energy gap wider than 2eV and has extremely high power, high voltage switching characteristics and high chemical, thermal and mechanical stability. This semiconductor material overcomes the limitations of silicon for high voltage high power devices. Due to wide band gap, high thermal conductivity and high mobility, SiC can be used to fabricate the high voltage high power devices.

SiC has the large band-gap and high thermal conductivity necessary for elevated temperature operation, mobilities that enable high-speed switching and low dynamic power loss. Switching speeds above 100 kHz are attainable with dynamic power losses reduced 5-10 times compared to silicon diodes.

The physical properties of SiC such as high electric field strength, high saturation drift velocity and high thermal conductivity has placed SiC at the centre of renewed focus of semiconductor material and device research amongst other wide energy gap semiconductors. SiC is an ideal semiconductor for high temperature, high frequency and high power electronic devices because of its various properties. Due to high thermal conductivity and breakdown electric field, the integration of the devices made from SiC is possible with higher package densities. The high breakdown fields of Silicon Carbide allow for drift regions that are eight to ten times thinner than Silicon high voltage devices which makes power devices made from silicon carbide feasible even in kilovolt range and beyond. So, the current handling capacity of these devices can be improved. More explicitly, due to the high Si-C bonding energy of about 5.0eV, SiC is resistant to high temperature and radiation.

Its intrinsic resistance to oxidation, corrosion and creep at high temperatures makes it suitable for harsh environment device applications. It is also an excellent heat sink because of its very high thermal conductivity. The combination of excellent semiconducting and mechanical properties therefore makes SiC the most promising material of choice for device application.

SiC provides several application opportunities :

- High voltage and power electronics applications such as lamp ballasts, motor control, automotive electronics, high-density high-frequency power supplies and smart-power application-specific integrated circuits.

- High-temperature sensor applications for aircraft engines, oil drilling and automotive electronics which has efficient fuel control and emission control.
- SiC offers the advantages of eliminating expensive cooling systems needed in industrial equipment essential to factories worldwide.

The first step in making silicon carbide semiconductor devices is the growing of the epitaxial layer using a process called chemical vapor deposition (CVD). The silicon carbide epilayers are produced in the CVD process by thermally decomposing silicon and carbon source gases (called precursors) onto boule-derived SiC substrates.

The SiC lattice consists of alternating planes of silicon and carbon atoms, and the stacking sequence of these planes defines different polytypes of the material identified by the repeating distance of the stacking sequence (e.g. 3C, 4H & 6H). The lattice constant in the basal plane is virtually identical for all polytypes, but important electrical properties such as band gap energy, electron mobility and critical field differ significantly between the polytypes.

## 1.2 SiC Structure

SiC is a group IV compound semiconductor. The main building block of the semiconductor material is a tetrahedron of C (Si) atom at the centre covalently bonded to four Si (C) atoms. The distance between two neighbouring Si or C atoms is 3.08 Å approximately and the distance between each pair of Si atom and C atom (i.e. Si-C bond length) is almost equal to 1.89 Å [1].

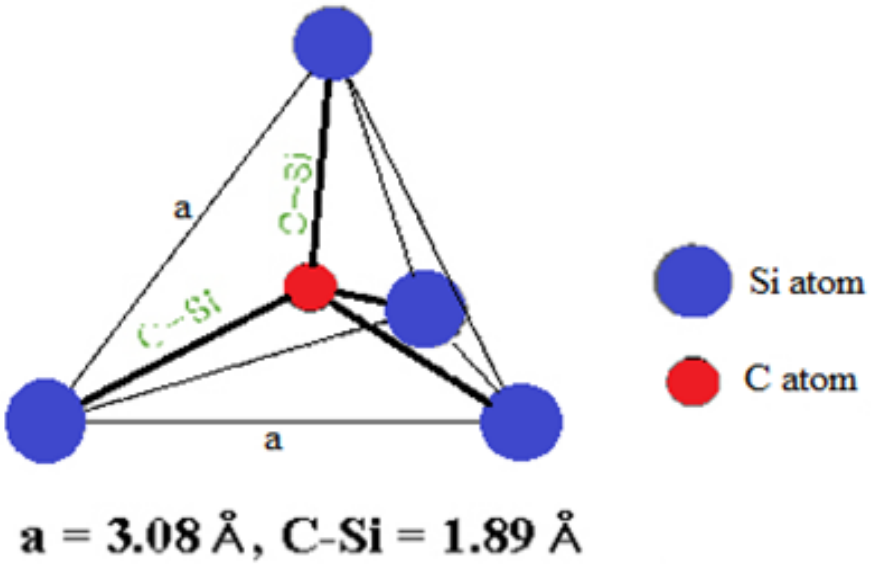


Figure 1.1: Si-C tetrahedral basic unit [1]

### 1.2.1 Silicon Carbide Polytypes

Silicon carbide occurs in many different crystal structures, called polytypes. Despite the fact that all SiC polytypes chemically consist of 50% carbon atoms covalently bonded with 50% silicon atoms, each SiC polytype has its own distinct set of electrical semiconductor properties. To date, SiC has more than 200 polytypes [2]. Among these, there is only one cubic polytype β-SiC or 3C-SiC. All the rest are α-SiC. 3C-, 4H- and 6HSiC are three stable single crystalline polytypes for device purposes. The most common polytypes of SiC presently being developed for electronics are 3C-SiC, 4H-SiC, and 6H-SiC. Furthermore, islands of 15R-SiC can be found on 4H-SiC and 6H-SiC wafers and small crystals of 2H-SiC have been grown. The difference between the polytypes is the staking order between the double layers of carbon and silicon atoms. In Figure.1.2, the stacking sequence is shown for the three most common polytypes 3C, 4H and 6H-SiC. If we assign a Si-C atom pair in an A-plane in a close packed lattice as A, and in the B-plane as B, and in the C-plane as C, then we can generate a series of lattice unit cells by variation of SiC plane stacking sequence along the principal crystal axis as in Figure1.2.

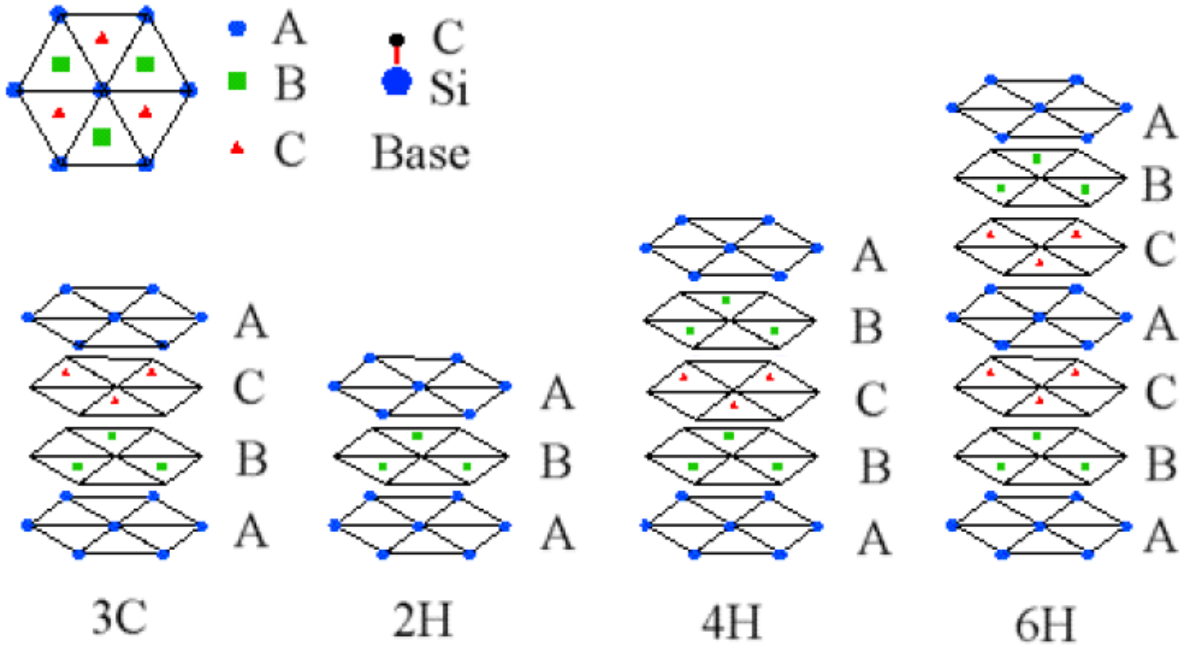


Figure 1.2: Stacking sequences of SiC polytypes [3]

The ABCABC... stacking, will give rise to the 3C-SiC zinc-blende lattice and ABAB... stacking on the other hand will produce the 2H-SiC wurtzite lattice. Other stacking sequences such as ABACABAC.. and ABCACB... will generate 4H-SiC and 6H-SiC lattice structures respectively. The number of atoms per unit cell varies from polytype to polytype, significantly affecting the number of electronic energy.

### 1.2.1.1 6H-SiC

6H-SiC has large anisotropy structure because of the long repletion length in the crystallographic lattice. The mobility of 6H-SiC in the perpendicular direction to the c- axis (commonly parallel to the surface) is four times higher than in the direction parallel to c- axis [4]. In comparison to Si, mobility in 6H-SiC is about 25% in the direction perpendicular to the c-axis and 7% in the direction parallel to it. The saturation velocity for 6H-SiC is $2\times10^7$ cm/s in the direction perpendicular to the c axis, but only $0.6\times10^7$ cm/s in the direction parallel to it.

### 1.2.1.2 4H-SiC

The 4H-SiC has low field mobility with a small anisotropy (20% higher in the direction parallel to the c-axis which is about half that of silicon [5-7]. The anisotropy in 4H-SiC depends on the electric field distribution and at high electric fields, the saturation velocity is 20% lower in the c-axis direction. 4H-SiC and 6H-SiC are the most common poly types

which have been characterized most thoroughly in literature so far. The transport properties are better for 4H-SiC and at present, this poly type forms the basis for most of the commercial electronics products [8]. 4H and 6H SiC have hexagonal lattice structure.

#### 1.2.1.3 2H-SiC

The substrate of 2H-SiC is not commercially available, but small mono-crystalline pieces have been grown successfully [9]. The performance of 2H-SiC is almost same as 4H-SiC in the direction perpendicular to the c-axis, but the mobility is better in the direction parallel to the c axis [10]. Research is under way in order to study this poly type at a greater depth.

#### 1.2.1.4 3C-SiC

3C-SiC is the only polytype with cubic lattice structure. Since this polytype can be grown on silicon substrates, the low cost, large-size 3C-SiC wafers are significantly used in microelectronic applications. Another advantage is that 3C-SiC does not have any stacking faults. 3C-SiC has larger electron mobility and saturation velocity than for 4H-SiC but has reduced hole mobility. The main disadvantage is that it has lower band-gap and breakdown field in comparison to other polytypes [8].

#### 1.2.1.5 15R-SiC

15R-SiC is very complex structure with 15 atomic layers ordered in a rhombohedral structure. A few years ago, much attention was given on 15R-SiC because it gave better performance experimentally as compared to the other polytypes when used as MOSFET [11]. The devices have been manufactured on 4H-SiC or 6H-SiC substrates, where pieces of 15R-SiC were found. Monocrystalline 15R- SiC wafers are however not a reality in the near future.

## 1.3 Properties of SiC

Owing to the differing arrangement of Si and C atoms within the SiC crystal lattice, each SiC polytype exhibits unique fundamental electrical and optical properties. Some of the more important semiconductor electrical properties of the 3C, 4H, and 6H SiC polytypes are given in Table.1. Even within a given polytype, some important electrical properties are non-isotropic, in that they are strong functions of crystallographic direction of current flow and applied electric field (for example, electron mobility for 6H-SiC). Dopant impurities in SiC can incorporate into energetically inequivalent sites. While all dopant ionization energies associated with various dopant incorporation sites should normally be considered for utmost accuracy, Table.1 lists only the shallowest reported ionization energies of each impurity.

Table 1.1 Comparison of electronic properties of SiC with Si, GaAs and GaN [12]

| | **Si** | **GaAs** | **GaN** | **6H-SiC** | **4H-SiC** | **3C-SiC** |
|---|---|---|---|---|---|---|
| Bandgap (eV) | 1.1 | 1.142 | 3.39 | 3 | 3.26 | 2.2 |
| Breakdown field @ $1017cm^{-3}$(MV/cm) | 0.6 | 0.6 | 3.3 | 3.2 | 3.0 | 1.5 |
| Electron mobility @$1016cm^{-3}$ (cm2/V-s) | 1100 | 6000 | 1000 | 370 | 800 | 750 |
| Hole mobility @$1016cm^{-3}$ ($cm^2$/V-s) | 420 | 320 | 200 | 90 | 115 | 40 |
| Saturated electron drift velocity (cm/s) | $10^7$ | $10^7$ | $2.5x10^7$ | $2x10^7$ | $2x10^7$ | $2.5x10^7$ |
| Intrinsic concentration, $n_i$ ($cm^{-3}$) | $1.5x10^{10}$ | $1.9x10^{-10}$ | $2.1x10^6$ | $2.3x10^{-6}$ | $8.2x10^{-9}$ | 6.9 |
| Thermal conductivity | 1.5 | 0.55 | 1.3 | 4.9 | 4.9 | 5 |

### 1.3.1 Mobility

The mobility characterizes how quickly an electron or hole can move through a semiconductor when pulled by an electric field. Due to random scattering within the crystal, the velocity does not increase linearly with electric field. The electron velocity rather quickly reaches an equilibrium mean-velocity proportional to the mobility and the electric field. The mobility in Silicon Carbide is somewhat lower in comparison to silicon. The low mobility in SiC devices is compensated by its ability to withstand high electric fields taking advantage of the higher carrier velocity. To some extent the mobility can be described using the same models as those used for silicon. The parameters for the mobility models are collected from measurements for a temperature dependent mobility model [13].

### 1.3.2 Saturation Velocity

At high electric fields, due to increased scattering the velocity becomes proportional to the electric field. The velocity saturates at $V_{sat}$, which is approximately twice the value for SiC than that for silicon. A high saturation velocity allows faster devices with shorter switching times.

### 1.3.3 Band Gap

A forbidden zone in the energy spectra for a crystal is known as band gap. Crystal is a metal without a band-gap and an insulator with a large band gap. A semiconductor has a band-gap up to a few eV. For some traditional semiconductors the band gaps are: 1.11eV for Si, 0.7eV for Ge, and 1.4eV for GaAs. Many of the favourable transport parameters in SiC are related to the large band-gap, which is of the order of 3eV. For such a large band gap the intrinsic carrier concentration (responsible for the thermal noise and also partly responsible for the leakage current) is negligible at temperatures up to 600°C. The minimum energy required to create an electron-hole pair is equal to the band-gap and in case of SiC, this energy falls within the 3eV range corresponding to a photon with wavelength close to 400 nm. SiC devices are thus also insensitive to the main part of the visible spectrum, which makes it suitable as a detector material for UV radiation with minimal noise from the visible background[14].

### 1.3.4 Critical Electric Field

With high electric field, the carrier energy increases and the probability of an impact ionization event increases as the energy exceeds the band-gap. In an impact-ionization event the carrier knocks out one electron from the valence-band thus creating an electron-hole pair (EHP) in turn. Now according to conservation of energy principle, the energy for the incident carrier is reduced by the band gap energy plus the initial energy for the created electron and hole. The critical electric field is related to the impact ionization rate, which increases as the carrier energy exceeds the band-gap value. The critical electric field for large band gap is thus about 10 times higher in SiC than for small band-gap materials such as Si and GaAs

### 1.3.5 Thermal Conductivity

Thermal conductivity is a very important quality in power semiconductor. For high power devices the thermal effects constitute one of the main limiting factor of the performance. One of SiC´s competitors is gallium nitride (GaN), which is a material with similar properties to those of SiC but gallium nitride has lower thermal conductivity than silicon (1.3 W/cmK) and silicon carbides. However, gallium nitride is often grown on SiC substrates, with its better thermal conductivity. Nevertheless, the GaN-SiC interface has lower thermal conductivity than GaN itself which leads to a degradation of the performance.

### 1.4 Advantages Of 3C-SiC

- The 3C-SiC has isotropic electron Hall mobility and in comparison to those of 4H and 6H polytypes, it is higher due to low density of interface states.
- This polytype can be grown on silicon substrates so, low cost, large-size 3C-SiC wafers are significantly used in microelectronic applications.
- Since 3C-SiC has smaller band gap, the interface states observed in 6H-SiC and 4HSiC, poor performance parameters are located in the conduction band and does not affect the transport properties of the channel.
- The 3C-SiC devices have lower specific junction capacitance in comparison to the 4H-SiC and 6H-SiC devices due to lower drift region doping which is an advantage for the high speed MOSFETs.

## 1.5 Applications of SiC Electronics

Silicon carbide is a wide band gap semiconductor which can be used in high power and high temperature electronics applications due to its high thermal conductivity and high breakdown electric field. Due to the physical and electronic properties of SiC, the devices fabricated from SiC can operate at higher temperatures and high power levels than those which are fabricated from silicon or GaAs. Although silicon based devices are primarily used in modern electronics, silicon is incapable of handling many special requirements. The devices which operate at high speeds, at high power levels and are to be used in extreme environments at high temperatures and high radiation levels require other material with wider band gap than that of silicon. Many space and terrestrial applications also have a requirement of wide band gap material. Due to high saturated drift velocity, silicon carbide also has great potential for high power and frequency operation. The wide band gap also allows for optoelectronic applications like blue light emitting diodes and ultra violet photodetectors [15].

- Silicon carbide is a popular abrasive in modern lapidary due to the durability and low cost of the material. It is used for its hardness in abrasive machining processes for manufacturing like grinding, honing, water-jet cutting and sandblasting. Particles of silicon carbide are laminated to paper to form sandpapers and the grip tape on skateboards [16].
- Silicon carbide is used as a support and shelving material in high temperature kilns like for firing ceramics, glass fusing, or glass casting. SiC kiln shelves are

considerably lighter and more durable as compared to traditional alumina shelves [17].

- Silicon-infiltrated carbon-carbon composite is used for high performance "ceramic" brake discs, due to its capablity to withstand extreme temperatures. The silicon reacts with the graphite in the carbon-carbon composite to form carbon-fiber-reinforced silicon carbide (C/SiC). These discs are used on some road-going sports cars, supercars, as well as other performance cars [18].
- Usage of SiC columns was originally intended to eliminate the requirement for the spark gap in a lightning arrester. Gapped SiC lightning arresters were used as lightning-protection tool and sold under GE and Westinghouse brand names, among others. The gapped SiC arrester has been largely displaced by no-gap varistors which use columns of zinc oxide pellets [19].
- The first LED action was demonstrated in 1907 using SiC and the first commercial LEDs were again based on SiC. The production of LEDs made from SiC was stopped because of the difference in efficiency due to the unfavourable indirect bandgap of SiC, whereas GaN has a direct bandgap which favours light emission. However, SiC is still one of the important LED components – it is a popular substrate for growing GaN devices, and it also serves as a heat spreader in high-power LEDs [20].
- Silicon carbide is a desirable mirror material for astronomical telescopes due to its low thermal expansion coefficient, high hardness, rigidity and thermal conductivity make. The growth technology (chemical vapour deposition) has been scaled up to produce disks of polycrystalline silicon carbide up to 3.5 meters in diameter, and several telescopes (like the Herschel Space Telescope) are already equipped with SiC optics [21].
- Silicon carbide fibers are used in measuring gas temperatures in an optical technique called thin filament pyrometry. It involves the placement of a thin filament in a hot gas stream. Radiative emissions from the filament can be correlated with filament temperature.

## 1.6 Silicon Carbide Devices

Silicon carbide has several unique properties which are useful for enhanced performance in devices made from silicon carbide. These properties include high breakdown field, wide band gap, lower thermal generation rate, and lower intrinsic carrier concentration. Different Sillicon Carbide Devices are as follows:

### 1.6.1 Schottky Barrier Diode

Schottky barrier diodes have lower resistance, faster response, and negligible transient reverse current during switching in comparison to p-n rectifiers. Moreover, the reverse saturation current of Schottky diodes is larger than that of p–n junction diodes. Hence, a Schottky diode requires less forward bias voltage to obtain a given current than p–n junction diode. Schottky diodes based on silicon carbide (SiC) are of special importance because of their high voltages and high temperatures handling capacity.

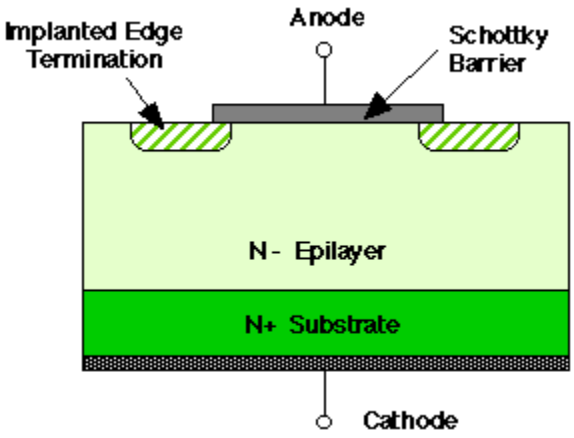


Figure 1.3: Cross section of an implant-edge-terminated Schottky barrier diode in SiC [22]

SiC have exceptional chemical and physical properties such as high thermal conductivity, a wide band gap, high breakdown field, high saturation velocity, and chemical stability. So, metal-SiC Schottky contacts are suitable for electrical devices for harsh environments such as high voltage rectifiers, UV radiation detectors, signal mixers, and high temperature gas sensor. The cross section of SBD is shown in Figure 1.3.

### 1.6.2 Silicon Carbide IMPATT Diode

Silicon carbide is an ideal semiconductor for the production of high-power microwave devices because of its high breakdown field. One device that benefit from the high

breakdown field of SiC is the IMPact ionization Avalanche Transit-Time (IMPATT) diode oscillator. [23]

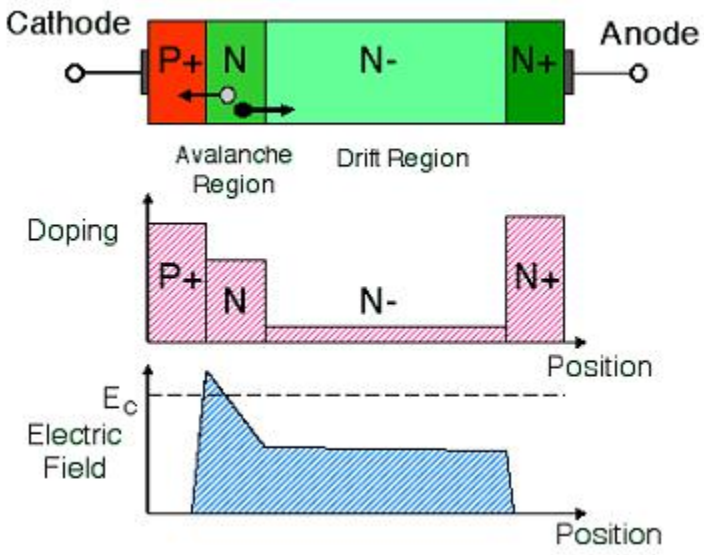


Figure 1.4: Cross section of SiC IMPATT diode [24]

IMPATT diodes give the highest RF power of any semiconductor microwave oscillator, and they are used for producing carrier signals for microwave transmission systems, mainly airborne and ground-based radar. IMPATT diodes operate from few GHz to few hundred GHz depending upon the design. The IMPATT diode has power-frequency product as the square of the critical field for avalanche breakdown times the electron saturation drift velocity. Electron-hole pairs are generated at the point of highest electric field (the "Avalanche Region"). Holes move toward the cathode, while electrons drift toward the anode, which induces a displacement current in the external circuit as they drift. Figure 1.4 shows the build up of microwave oscillations in the diode current and voltage when the diode is embedded in a resonant cavity and biased at breakdown.

### 1.6.3 Charge Coupled Devices

Charge coupled devices (CCDs) are linear shift registers which are formed when a series MOS plates are closely spaced on the surface of a semiconductor. When bias voltage is applied to the MOS plates, the localized potential wells are created in the semiconductor under each plate. Charge packets are confined in the potential wells and under the influence of appropriate clocking waveforms applied to the gates, packets can be shifted along the surface. The application of silicon CCDs is its use in image sensing, particularly in digital still cameras and hand-held video cameras. Since wide band gap of makes it transparent to

visible light which results in an ultraviolet (UV) sensor which is virtually blind to solar radiation, it can be used as specialized image sensor which has many applications in aerospace research, UV astronomy and in military systems. The source and drain junctions and the buried n-type channel are formed in this structure by nitrogen ion implantation and by high temperature annealing, the implants are activated. By using the optimized conditions identified in MOS investigations, gate oxide is grown thermally. Then a layer of polysilicon for the first-level gates is deposited and doped the poly with phosphorus. The polysilicon is organized in a pattern by reactive ion etching and oxidized to form a passivation layer. Then a second layer of polysilicon is deposited and doped to form the second-level gates.[23]

### 1.6.4 Silicon Carbide Non-volatile Memory Devices

4H silicon carbide is a single-crystal semi conducting material and has a band gap of 3.26 eV. This wide band gap leads to an extremely low value for the intrinsic carrier concentration in room temperature, about 16 orders of magnitude lower than silicon. Leakage currents in SiC are negligible because thermal generation varies directly with the intrinsic carrier concentration [25].

### 1.6.5 Digital CMOS Integrated Circuits in SiC

CMOS technology is appealing for digital logic as it consumes low power, full rail-to-rail output swing, and greater noise margins than NMOS circuits. CMOS also gives active current sources for linear applications. Development of CMOS technology in SiC is expected to deliver low power, high temperature circuits as well as reliable control circuitry for smart power integrated circuits. In this process, an implanted n-well is used and oxides are deposited on it, but due to other processing problems the PMOSFETs exhibited a very high threshold voltage. This device is fabricated by using an implanted p-well and thermally grown oxide. The sequence of fabrication is as follows [26]:

**1.** P-wells are formed on n-type epitaxial layers doped at $8x10^{15}cm^{-3}$ by boron implantation. Then, Al and N are implanted through polysilicon masks for the formation of P+ and N+ source/drain regions, respectively.

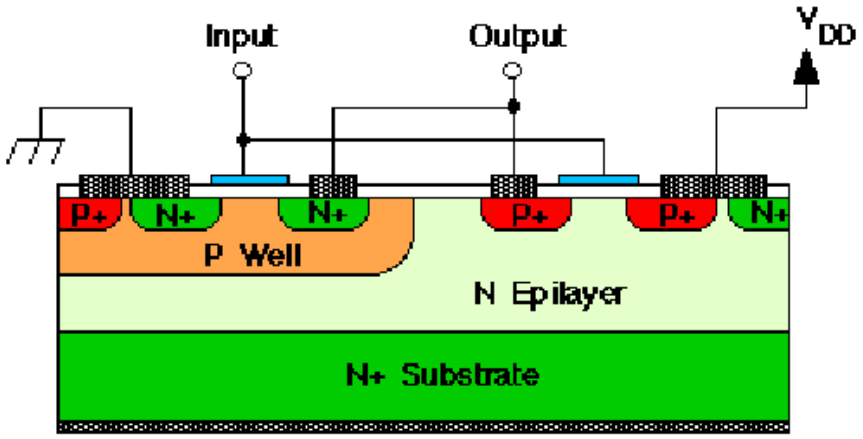


Figure 1.5: Cross section of a CMOS inverter in the implanted p-well process [26].

**2.** NMOSFETs are formed on p-wells and PMOSFETs are formed on n-type epilayers. Then, annealing of implants is done at $160^0$C for 40 minutes in argon, followed by an $115^0$C, 2 hour wet oxidation to form a 40 nm gate oxide layer.

**3.** Then polysilicon is deposited and patterned for the formation of the gates. Al-Ni is used for p-type ohmic contacts and Ni for n-type contacts. Then a layer of silicon oxynitride is deposited as an inter-metallic dielectric.

**4.** $V_i$ are opened and interconnected metal is deposited and patterned.

### 1.6.6 3C-SiC Power MOSFETs

SiC has breakdown electric field approximately 8 times higher than that of silicon. This leads to the designing of power switching devices having correspondingly higher blocking voltages than their silicon counter parts. Moreover, the specific on resistance (i.e. resistance-area product) of a power device is inversely proportional to the cube of the breakdown field, so the SiC power MOSFETs have 100-200 times lower on-resistance in comparison to devices made from silicon.[27]

# CHAPTER 2

# SCHOTTKY BARRIER DIODE OF SiC

The Schottky diode (named after German physicist Walter H. Schottky; also known as hot carrier diode) is a semiconductor diode with a low forward voltage drop and a very fast switching action. There is a small voltage drop across the diode terminals when current flows through a diode. A normal silicon diode has a voltage drop between 0.6–1.7 volts, while a Schottky diode has a voltage drop approximately 0.15–0.45 volts. This lower voltage drop gives higher switching speed and better system efficiency.

A metal–semiconductor junction is formed between a metal and a semiconductor, forming a Schottky barrier (instead of a semiconductor–semiconductor junction as in conventional diodes). Typically molybdenum, platinum, chromium or tungsten metals are used and the semiconductor would typically be N-type silicon. The metal side acts as the anode and N-type semiconductor acts as the cathode of the diode. This Schottky barrier leads to very fast switching and low forward voltage drop.

## 2.1 3C-SiC Schottky Barrier Diode

In the area of power semiconductors, Si devices can usually provide either high speed (Schottky barrier diodes) or high breakdown (p-i-n diodes), but not both, while devices made from SiC can provide both of these characteristics. Schottky diodes constructed from silicon carbide have a much lower reverse leakage current as compared to silicon Schottky diodes, and higher reverse voltage.

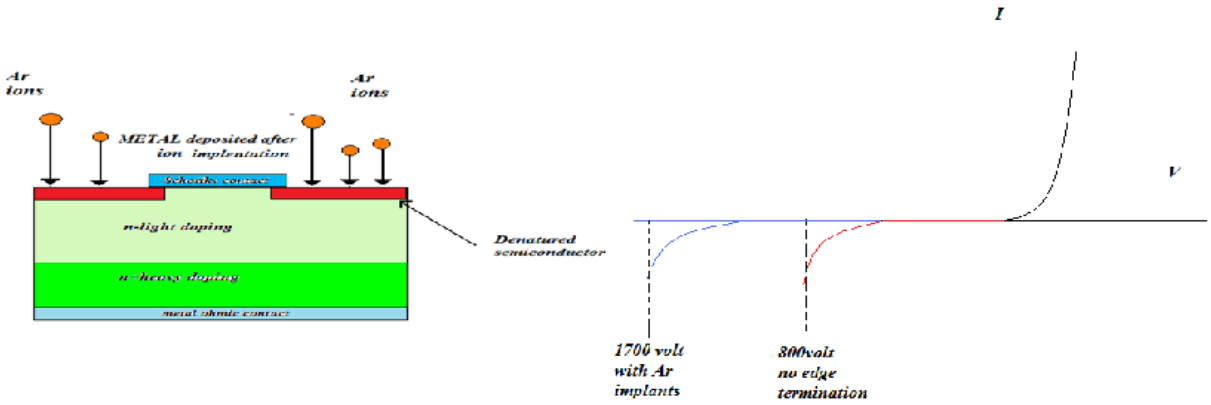


Figure 2.1: Cross-section of SBD and V-I characteristic [28]

A lightly doped n-type blocking layer is grown on a SiC substrate by chemical vapour deposition. The doping and thickness of the epilayer are selected so that the desired blocking voltage is achieved. On the top surface of the blocking layer an edge termination ring is implanted at the surface and then the Schottky metal is deposited to form Schottky junction. The edge termination ring is required to prevent field crowding at the edge of the metal in the blocking state; otherwise blocking voltage would be significantly reduced. Two types of edge termination rings used are resistive termination extension (RTE) and junction termination extension (JTE).

Silicon Carbide (SiC) Schottky Barrier Diode (SBD) was the first power device made from SiC that was demonstrated. It was studied as early as 1974. As single crystalline SiC material became commercially available throughout the years and also its quality improved steadily, substantial amount of work and study has been done on SiC SBDs and also on Merged P-i-N Schottky diodes (MPS) and Junction Barrier Schottky (JBS) diodes. Schottky contacts on 3C, 6H and 4H SiC were made with a large variety of metals and their performance was studied.

## 2.2 Operation

Forward current in a Schottky diode is because of injection of majority carrier from the semiconductor to the metal. Reverse current is also due to majority carriers which overcome the Schottky barrier and it is dependent on temperature. The Schottky diode has two different metal contacts on a semiconductor, a Schottky (rectifying) contact and an ohmic contact. A metal can be characterized by a work function ($\Phi_m$), the minimum energy needed to remove an electron

from the metal to the vacuum level. The barrier between the metal and semiconductor can be seen on energy band diagram. In an energy band diagram, metal and semiconductor are aligned using the same vacuum level as shown in Figure 5 and Figure 6. When the metal and semiconductor are brought close to each other, then there will be a barrier established between the metal and semiconductor interface. The height of barrier $\Phi_B$ is the energy required to free up an electron from metal (Φm) minus the energy required to remove the electron from n-type semiconductor material (called electron affinity, χ) which is given by

$$\Phi_B = \Phi_m - \chi \qquad 2.1$$

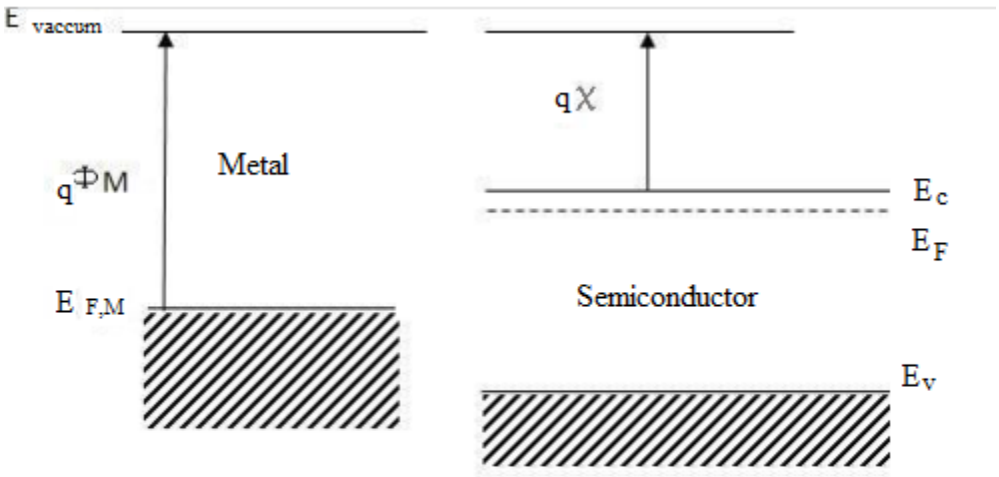


Figure 2.2: Energy band gap of M-S before contact [29]

Whenever metal and semiconductor align together, only a small number of electrons have sufficient amount of energy required to get over the barrier and cross to the metal. When a bias voltage is applied to the junction, the height of Schottky barrier becomes lower or higher. When the barrier is large, the electrons require more energy to cross the barrier and the contact has rectifying behaviour also called Schottky contact. When the barrier is small, electrons can move freely from the semiconductor to the metal and the contact is called ohmic contact.

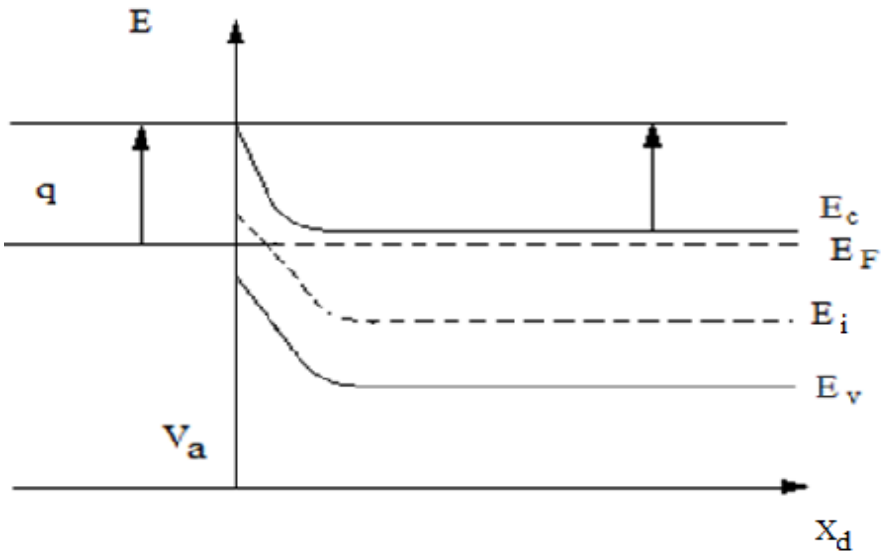


Figure 2.3: Energy band gap of M-S after contact and before thermal equilibrium [29]

A positive charge is left behind when electrons leave the semiconductor due to the ionized donor atoms. Electrons flow into the metal until equilibrium is established between the diffusion of electrons from the semiconductor into the metal and the drift of electrons caused by the field generated by ionized impurity atoms. This equilibrium of flow of electrons is called thermal equilibrium.

## 2.3 Forward and Reverse bias

Schottky Barrier Diode is a unipolar device and the flow of current is dominated by only one carrier, majority carrier. When a positive bias voltage is applied to the metal, the Fermi energy of the metal is lowered with respect to Fermi energy in the semiconductor. This leads to a smaller potential drop across semiconductor. The balance between diffusion and drift of electrons is disturbed and more electrons start diffusing towards the metal than the number drifting into the semiconductor. This diffusion results in a positive current through the junction at a voltage comparable to the built in potential. When a negative bias voltage is applied, the Fermi energy of the metal is increased with respect to the Fermi energy in the semiconductor. The potential across the semiconductor increases, resulting in a larger depletion region width and a larger electric field at the interface.

The barrier, which limits the flow of electrons to the metal, is unchanged so that the barrier, independent of the applied voltage, restricts the flow of electrons. Therefore, the metal

semiconductor junction with positive barrier height has a rectifying behaviour. A large current exist under forward bias, while under reverse bias, no current exist. Hence, the potential across the semiconductor is equal to the built in potential minus the applied voltage.

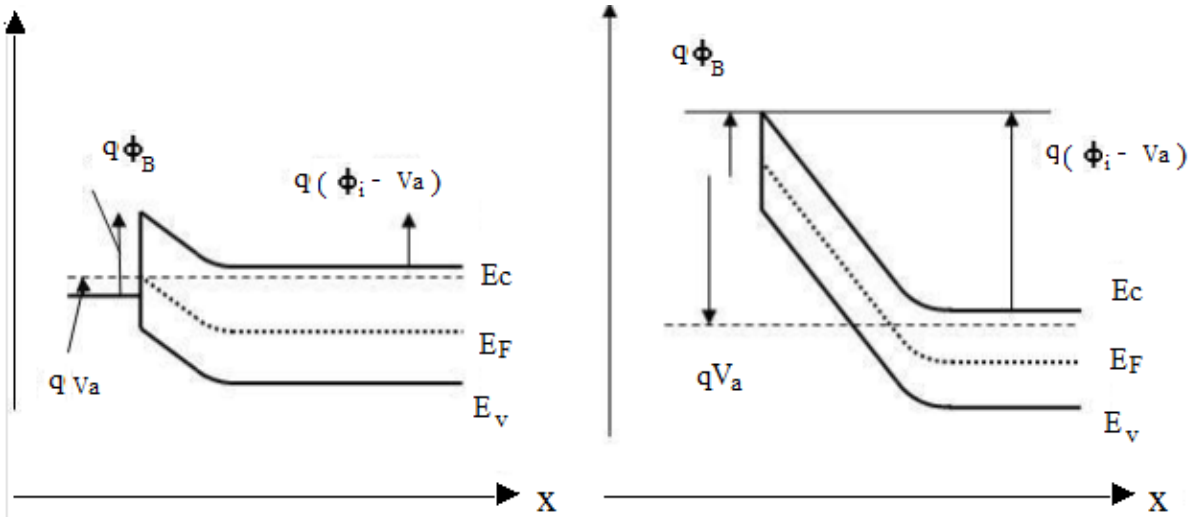


Figure 2.4: Energy band diagram of (a) forward biased (b) reverse biased M-S junction [29]

## 2.4 Breakdown Voltage in a Schottky Barrier Diode

An important feature of power devices is the blocking voltage that the device can handle before "breaking down". The breakdown of a device is characterized by the impact ionization of carriers within the depletion region. When larger reverse bias voltage is applied, the peak electric field increases inside the device as established. As the electric field increases, the acceleration of the carriers being swept through the depletion region is increased. This acceleration will increase to a level where the carrier has enough energy to ionize an atom in the semiconductor lattice, in other words, generate an electron-hole pair. This is known as impact ionization. Impact ionization can begin to occur unrestricted if the electron-hole pair that is originally generated through impact ionization gains enough energy to impact ionize another lattice site, and the newly created electron-hole pair causes impact ionization at another site, and so on. As newly created electron-hole pairs generate their own new electron-hole pairs, an avalanche of electron-hole pair generation begins. This exponentially increasing avalanching causes the current to quickly tend towards negative infinity. As such, this snowball effect of electron hole pair generation is named avalanche breakdown. This takes place at the breakdown voltage, $V_{bd}$, which can be found as

$$V_{bd} = \frac{K_s \varepsilon_o E_{cr}^2}{2qN_D} \qquad 2.2$$

where, $E_{cr}$ is the critical electric field and $N_D$ is the doping of the substrate or epi-layer, provided the epilayer is not punched-through. This is the simplest way of defining breakdown. For a more rigorous derivation, the reader is referred to [30]

## 2.5 Literature Survey

It was in 1938 that German physicist Walter H. Schottky created a theory that illustrated the rectifying behaviour of a metal-semiconductor contact as dependent on a barrier layer at the surface of contact between the two materials. The metal semiconductor diodes i.e. Schottky Barrier diodes were later fabricated on the basis of this theory.

Mohit Bhatnagar and B.J. Baliga in March 1993 showed theoretically that an ideal SiC Schottky rectifier can provide a breakdown voltage as high as 5000V with a forward voltage drop of only 3.85V at 300°K for a current density of 100Amps/$cm^2$

In 1993, high voltage Schottky diodes were fabricated on 3C-SiC films grown on Si substrates by A. J. Steckl and J. N. Su. A Ni metallization process was developed to fabricate both rectifying and ohmic contacts to SiC by controlling the post annealing temperature. A high breakdown voltage (>150V) was obtained at room temperature from the SiC Schottky diode. The Ni-SiC Schottky junction showed a thermal resistance for temperatures as high as 600°C. This technology has good potential for monolithic integration of SiC high power devices and Si integrated circuits [31].

In 1994, Praveen Shenoy, Akira Moki, B.J.Baliga, Dev Alok**,** K.Wongchotigul and M.Spencer reported the characteristics of vertical Schottky barrier diodes (SBD) fabricated on N /N+ 3C-SiC grown on $N^+$Si substrate. The diodes exhibited a soft breakdown; at - 85 V which was the highest reported breakdown voltage for 3C-SiC SBD's. The barrier height of the Pt Schottky contact was determined to be ~0.85 eV. The low forward voltage drop of as-deposited Pt SBD's (~0.85 V at 100 A/$cm^2$) demonstrated that the $N^+$SiC/$N^+$Si heterojunction is highly conductive. The specific resistance of the heterojunction ($R_{on,HJ}$) was experimentally measured and an upper bound of $8x10^{-6}cm^2$ was obtained. $R_{on,HJ}$ was also extracted by one dimensional numerical simulations to be ~$8x10^{-6}cm^2$. These low values for $R_{on,HJ}$, demonstrated that vertical power device structures are feasible on 3C-SiC grown on Si [32].

In 1995, R. Raghunathan, D. Alok, and B. J. Baliga reported the characteristics of 4H-SiC Schottky barrier diodes with breakdown voltages upto 1000 V for the first time. The diodes showed excellent forward I-V characteristics with a forward voltage drop of 1.06 V at an on-state current density of 100 $A/cm^2$. The specific on-resistance for these diodes was found to be low (2 x $10^{-3}$ ohm-$cm^2$ at room temperature) and showed a $T^{1.6}$ variation with temperature. Titanium Schottky barrier height was determined to be 0.99eV independent of the temperature. The breakdown voltage of the diodes was found to decrease with temperature [33].

In 1998, Carl-Mikael Zetterling, Fanny Dahlquist, Nils Lundberg, Mikael oè Stling, Kurt Rottner and Lennart Ramberg fabricated junction barrier Schottky (JBS) diodes in 6H SiC and characterised electrically. This device was demonstrated in silicon technology and it had the advantage of a low forward voltage drop comparable to that of Schottky diodes, as well as a high blocking voltage and low reverse leakage current of a pn junction. This was especially attractive for wide bandgap materials such as SiC in which pn junctions have a large forward voltage drop. These devices were capable of blocking up to 1100 V with a leakage current density of 0.15 $Acm^{-2}$, limited by the leakage when the drift region was fully depleted, or breakdown of the SiC material itself. The forward conduction was limited by an on-resistance of 20 mΩ-$cm^2$, resulting in forward voltage drops of 2.6 V at 100 $Acm^{-2}$ [34].

In 2000, G. Brezeanu, M. Badila, B. Tudor, J. Millan, P. Godignon, Marie Laure Locatell, J. P. Chante, G. Amaratunga, F. Udrea, A. Mihaila presented an accurate modeling and complete parameters extraction of the forward characteristics of the Ni/6H-SiC Schottky barrier diodes (SBD) for high level current densities. The high level injection effects of the excess majority carriers and current dependence of the series resistance were described in the model. Direct extraction of the large bias SBD parameters was carried out. A very good agreement between the simulated forward curves using extracted parameters and measured data up to 500 $A/cm^2$ was obtained [35].

In 2001, Gheorghe Brezeanu, Marian Badila, Bogdan Tudor, José Millan, Philippe Godignon, Florin Udrea, G. A. J. Amaratunga and Andrei Mihaila fabricated Ni Schottky rectifiers on 2.7x$10^{16}$ $cm^{-3}$ n-type 6H-SiC epilayer using an effective edge termination based on an oxide ramp profile around the Schottky contact. Several anneals of the Schottky contacts were experimented. In particular, the diodes annealed at $900^0$C showed excellent reverse

characteristics with a nearly ideal breakdown at about 800 V. Forward characteristics follow the thermionic emission theory with the ideality factor close to one at low biases. An accurate analytical model and complete parameter extraction of the forward characteristics of the Ni/6H-SiC Schottky barrier diodes (SBDs) for low and high-level current densities were presented. The model takes into account the high-level injection effects and the current dependence of the series resistance. Direct extraction of the SBD parameters was carried out. A very good agreement between the simulated forward curves using extracted parameters and measured data up to 500 $A/cm^2$ was obtained [36].

In 2005, X. Jorda, D. Tournier, M. Vellvehi, A. Perez, R. Perez, P. Godignon, J. Millan compared the performance of the commercially available and recently fabricated Schottky Barrier Diode of breakdown voltage of 1.2 kV with the Si diodes at high temperature. It was found that for a rated breakdown voltage of 1.2 kV, SiC Schottky diodes offer better performances in terms of switching time and recovery charge than PN-Si ultra-fast diodes, although they showed slightly higher forward voltage drops. Lower reverse leakage current was obtained using Ni instead of Ti for the Schottky contact [37].

In 2006, F. Bjoerk, J. Hancock, M. Treu, R. Rupp and T. Reimann discussed silicon Carbide as energy efficient wide band gap device, which showed that SiC Schottky diodes allowed up to a 25% reduction in losses in power supplies for computers and servers when used in the power factor correction circuit. For motor control, SiC Schottky diode allowed a >35% reduction in losses as demonstrated for a 3HP motor drive [38].

In 2009,Jens Eriksson, Ming Hung Weng, Fabrizio Roccaforte, Filippo Giannazzo, Stefano Leone, Vito Raineri studied the electrical characteristics of Au/3C-SiC Schottky diode as a function of contact area. While the larger diodes were characterized by conventional current-voltage measurements, conductive atomic force microscopy was used to perform current-voltage measurements on diodes of contact radius down to 5μm. The results show that the Schottky barrier height increases when the contact area reduced, and for the smallest diodes the value approaches the ideal barrier height of the system. The results were correlated with defects in the 3C-SiC and an analytical expression was derived to describe the dependence of the barrier height on the defect density [39].

In 2009, R. Talwar and A.K. Chatterjee gave a method to theoretically calculate current-voltage characteristics of Schottky barrier diode defined by the diode equation, using iteration

method and C++ programming. The diode equation was split into two functions. A set of values of current and voltages was generated using C++ program. The analysis has been made using 4H-SiC diode with contacts of Nickel, Titanium & Gold [40].

In 2010, W. Janke and A. Hapka measured isothermal and nonisothermal DC characteristics of SiC Schottky barrier diodes. Various electro-thermal models for I-V characteristics calculation were proposed. The calculations of non-isothermal characteristics of SiC SBD's in the wide range of forward voltage were done. The self-heating phenomenon, as an electro thermal positive feedback is discussed in this work. The critical current and junction temperature estimation for SiC SBD is also explained [41].

In 2011, the transport properties of metal/3C-SiC interfaces were monitored employing a nanoscale characterization approach in combination with conventional electrical measurements by Jens Eriksson, Fabrizio Roccaforte, Sergey Reshanov, Stefano Leone, Filippo Giannazzo, Raffaella LoNigro, Patrick Fiorenza, Vito Raineri. In particular, using conductive atomic force microscopy allowed demonstrating that the stacking fault is the most pervasive, electrically active extended defect at 3C-SiC(111) surfaces, and it can be electrically passivated by an ultraviolet irradiation treatment. For the Au/3C-SiC Schottky interface, a contact area dependence of the Schottky barrier height (FB) was found even after this passivation, indicating that there are still some electrically active defects at the interface. Improved electrical properties were observed in the case of the Pt/3C-SiC system. In this case, annealing at 500°C resulted in a reduction of the leakage current and an increase of the Schottky barrier height (from 0.77 to 1.12 eV). A structural analysis of the reaction zone carried out by transmission electron microscopy [TEM] and X-ray diffraction showed that the improved electrical properties can be attributed to a consumption of the surface layer of SiC due to silicide ($Pt_2Si$) formation. The degradation of Schottky characteristics at higher temperatures (up to 900°C) could be ascribed to the out-diffusion and aggregation of carbon into clusters, observed by TEM analysis [42].

In 2012, HOYA Corporation has succeeded in raising the SiC growth rate to more than 50 times the conventional rate, using a newly developed SiC fabrication process. With this new process, large monocrystal 3C-SiC substrates (at least 200 micro-meters thick after removing the Si base layer) can be manufactured. These can then be handled using the same processes that are applicable to conventional Si substrates. Thus, HOYA's 3C-SiC substrate has the

same geometry as typical Si wafers, and can be used in conventional Si semiconductor device production lines without hardware modifications [43].

In 2013 a novel direct wafer bonding technique has been reported; Si wafers to polycrystalline silicon carbide carrier wafers. The purpose of this work is to provide a platform for 3C-SiC epitaxial growth above the wafer bonded Si wafers. 3C-SiC epitaxial layers have been grown by conventional chemical vapour deposition techniques above Si/SiC structures. All of these 3C-SiC epitaxial layers are highly crystalline in nature [44].

In 2013, an analysis of 4H-SiC power Schottky Barrier Diodes (SBDs) was done by K. Shenai which shows that these devices can be operated well below their true avalanche breakdown potential. It was found that the breakdown voltage ratings of these devices are smaller nearly by a factor of 2 due to increased leakage current caused by drift-region punch-through. A simple analysis is presented to determine the de-rating factor of SiC power SBDs using the information provided in the manufacturer's data sheets [45].

In 2013, Shamim Ahmed, H. Alan Mantooth, Mihir Mudholkar and Ranbir Singh presented a physics based compact model for SiC Junction Barrier Schottky (JBS) diodes which features a comprehensive physical description of the DC and CV behaviour of SiC JBS diodes. For the first time, modeling of leakage current for JBS diode in circuit simulation is done. The model includes temperature scaling of its parameters to enable modeling of the diodes over a wide range of temperature (25 °C to 175 °C) [46].

In 2014, Yan Liu, Chao Zhang, Zhitang Song, Bo Liu, Guanping Wu, Jia Xu, Lianhong Wang, Lei Wang, Zuoya Yang, and Songlin Feng proposed a cost-effective fabrication of Schottky-barrier (SB) diode steering element for low power phase-change memory (PCM) application. While superior drivability in conventional PN diode array, Schottky Barrier diode array with 0.0193-$\mu m^2$ ($5F^2$), performing higher switching speed, sufficient drive current density of ~26.30 mA/$\mu m^2$, disturbance immunity, and lower power consumption has been manufactured under 40-nm standard complementary metal oxide semiconductor technology. Simultaneously, different performance specifications, including integration scheme, $J_{ON}/J_{OFF}$ ratio, temperature characteristics, and scalability have been studied in detail and compared in two categories of accessing diode arrays. It demonstrates that the scaled Schottky Barrier diode array is suitable for full operation of PCM [47].

# CHAPTER 3

# THEORETICAL ANALYSIS

Usually the doping profiles used by the semiconductor industry commercially are non-linearly graded doping profile inside semiconductor layer. These profiles usually adopt either Gaussian profile or complementary error function profile (erfc). Here Gaussian profile has been used for the analysis. The profile can be generated by ion implantation from the base of the device. The carrier concentration decreases upwards from the base as we reach the contact.

In theoretical analysis of 3C-SiC Schottky Barrier Diode using Gaussian profile, the behaviour of breakdown voltage and depletion width with respect to the peak carrier concentration $N_0$ and constant m have been studied.

## Doping Profile

The doping profile used here in Schottky Barrier diode is Gaussian profile. The carrier concentration is maximum at the base of the device decreasing upwards at the contact. The equation to this profile may be written as:

$$N(x) = N_0 e^{-\left(\frac{h-x}{m}\right)^2} \qquad 3.1$$

Where, $N_0$ is peak concentration, m is constant, h is the device height (200μm) and x is the distance from the contact.

Here different Gaussian profiles have been generated with different values of peak concentration $N_0$ and constant m. $N_0$ has been varied from $10^{15}$ $cm^{-3}$ to $10^{18}$ $cm^{-3}$.

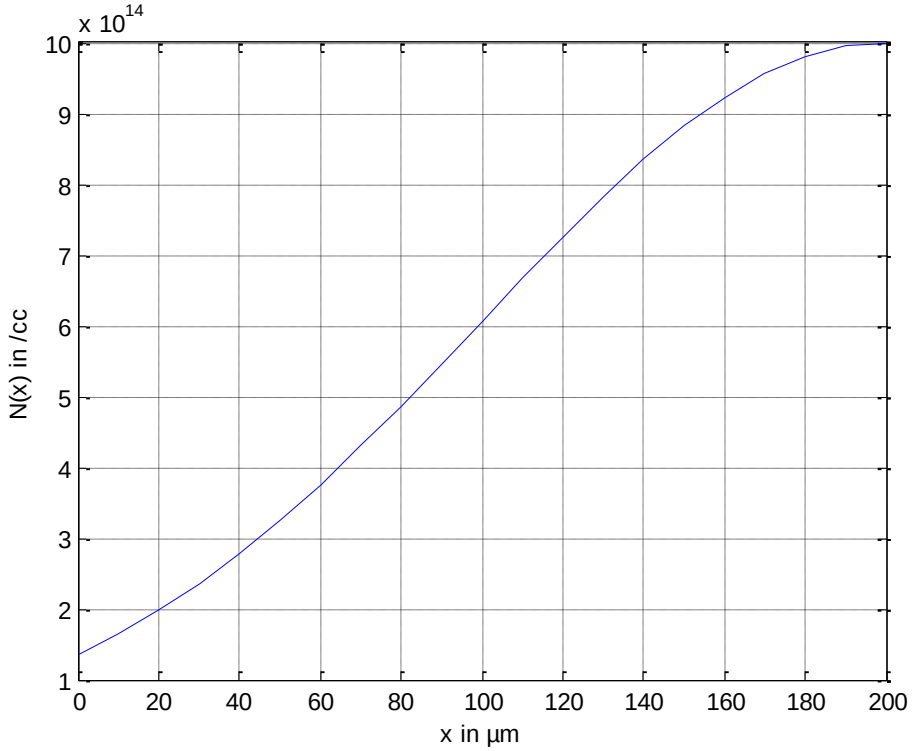


Figure 3.1 Profile1-Variation of carrier concentration N(x) with x with peak concentration $N_0=10^{15}$ $cm^{-3}$ and constant $m=100x10^{-4}cm$

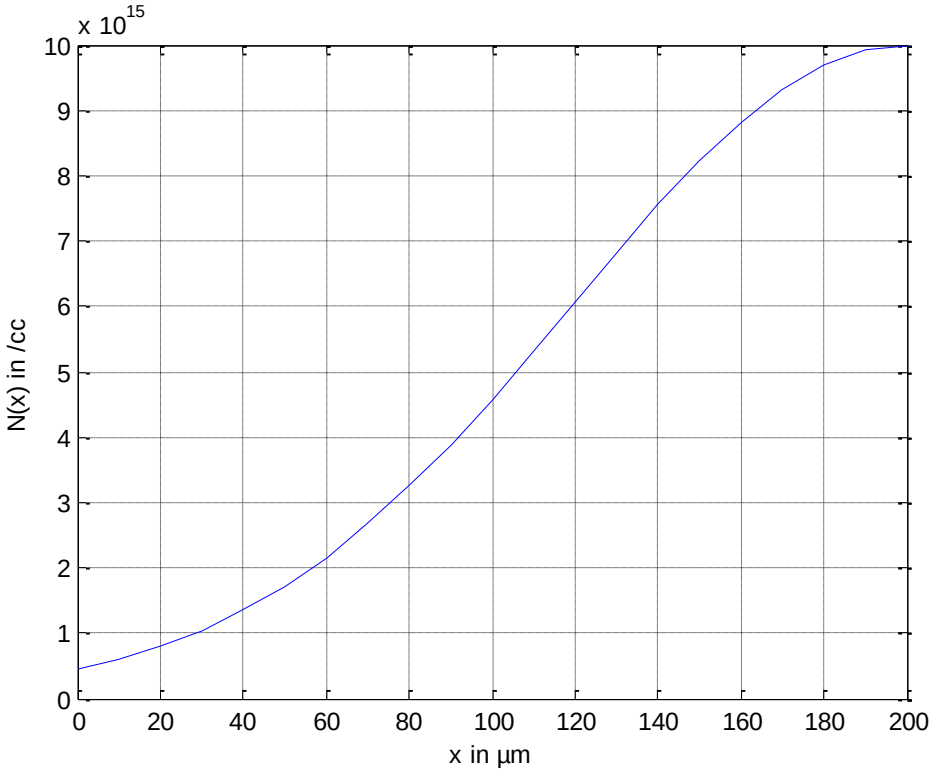


Figure 3.2 Profile2-Variation of carrier concentration N(x) with x with peak concentration $N_0=10^{16}$ $cm^{-3}$ and constant $m=80x10^{-4}cm$

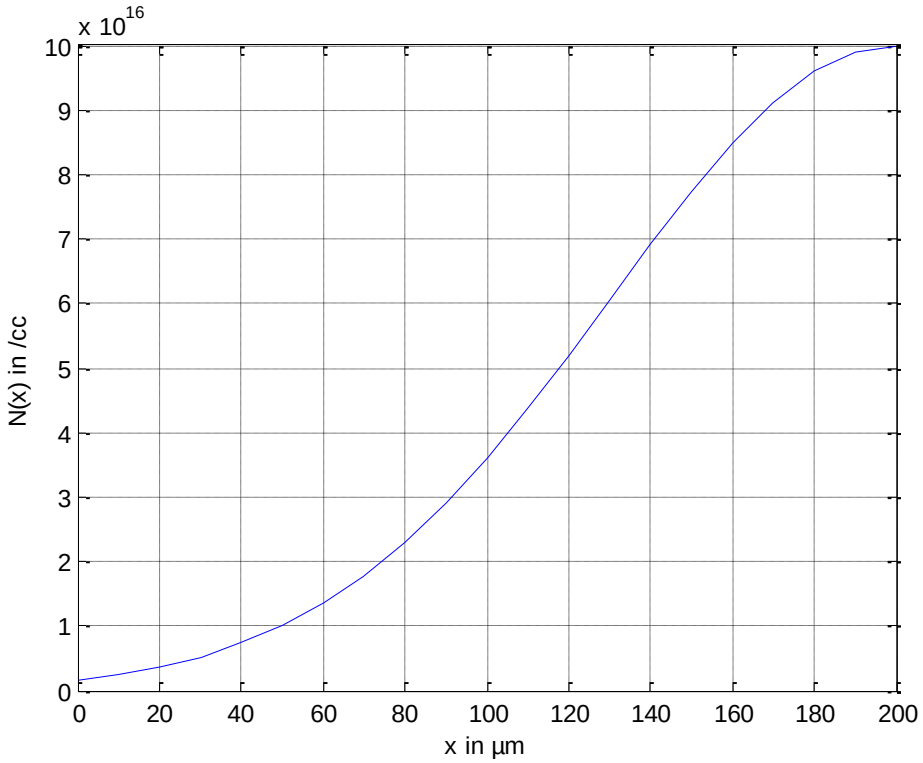


Figure 3.3 Profile3-Variation of carrier concentration N(x) with x with peak concentration $N_0=10^{17}$ $cm^{-3}$ and constant $m=70x10^{-4}cm$

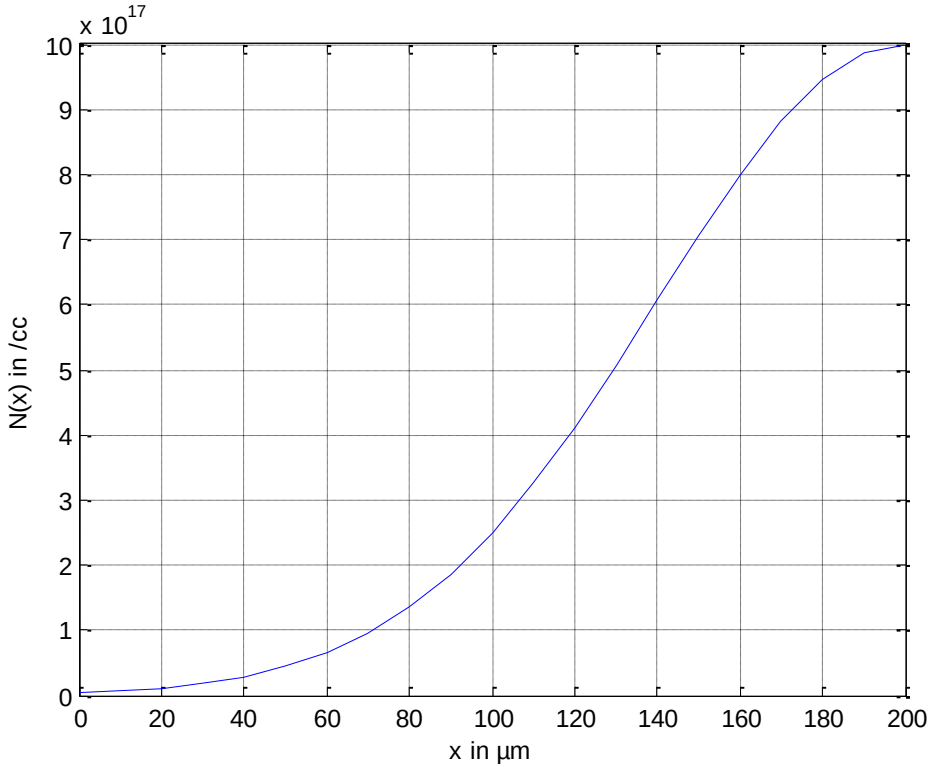


Figure 3.4 Profile4-Variation of carrier concentration N(x) with x with peak concentration $N_0=10^{18}$ $cm^{-3}$ and constant $m=60x10^{-4}cm$

## Equation for Obtaining the Depletion Region Width 'W'

The depletion region width at any given reverse voltage, $V_R$ can be obtained by solving the Poisson's equation for the system. Hence, for the Gaussian function G(x), the Poisson's equation becomes [48]

$$-\frac{\partial^2 V}{\partial x^2} = \frac{e}{\varepsilon_s} N(x) = \frac{eN_0 e^{-\left(\frac{h-x}{m}\right)^2}}{\varepsilon_s} \quad 3.2$$

On solving the above equation, we get

$$-V(x) = \frac{eN_0}{\varepsilon_s}\left[\frac{x^4}{12m^2} - \frac{hx^3}{3m^2} - \frac{x^2}{2}\left(1 - \frac{h^2}{m^2}\right)\right] \quad 3.3$$

At x=W, the depletion region width under a reverse bias $V_R$, then

$$V(W) = V_{bi} + V_R \quad 3.4$$

where $V_{bi}$ is the built in potential.

Substituting x=W and since $V_{bi} << V_R$, $V(W) \approx V_R$ and simplifying gives:

$$\frac{W^4}{12m^2} - \frac{hW^3}{3m^2} - \frac{W^2}{2}\left(1 - \frac{h^2}{m^2}\right) - \frac{\varepsilon_s V_R}{eN_0} = 0 \quad 3.5$$

The above equation is used for calculating the depletion region width. The calculations are done using MATLAB. Since this is fourth order equation, we get four solutions of depletion region width. Out of these four solutions, the most appropriate value of depletion width has been taken.

## Equation for Breakdown Voltages

In the present work, punch through breakdown voltage has been studied. The highest value of reverse voltage $V_R$ in eq. (3.5) at which maximum depletion region width is obtained for a given value of constant m gives the value of punch through breakdown voltage.

# CHAPTER 4

## CALCULATIONS AND RESULTS

The calculations have been done to obtain the values of depletion width for different reverse voltages $V_R$ using equation 3.5. The highest value of voltage $V_R$ at which maximum depletion width is attained for a given value of m gives punch through voltage.

Permittivity of free space $\varepsilon_o=8.854x10^{-14}$ $(\Omega cm)^{-1}sec$

Permittivity of 3C-SiC semiconductor $\varepsilon_s=9.7\ \varepsilon_o$

Electronic charge $e=1.6x10^{-19}$ coulomb

Device height h=200μm

Table 4.1-4.4 shows the depletion width calculated for different reverse voltages for the four profiles discussed above.

Table 4.1 Results of depletion width and reverse voltage for profile 1 (Figure 3.1).
$N_0=10^{15}\ cm^{-3}$, $m=100x10^{-4}$ cm

| Reverse Voltage $V_R$(kV) | Depletion Width W(μm) |
|---|---|
| 1 | 20 |
| 2 | 29 |
| 3 | 36 |
| 4 | 42 |
| 5 | 47 |
| 6 | 52 |
| 7 | 57 |
| 8 | 62 |
| 9 | 67 |
| 10 | 71 |
| 15 | 92 |
| 20 | 112 |
| 25 | 133 |
| 30 | 156 |
| 35 | 184 |

| | |
|---|---|
| 37 | 198 |
| 37.2 | 200 |

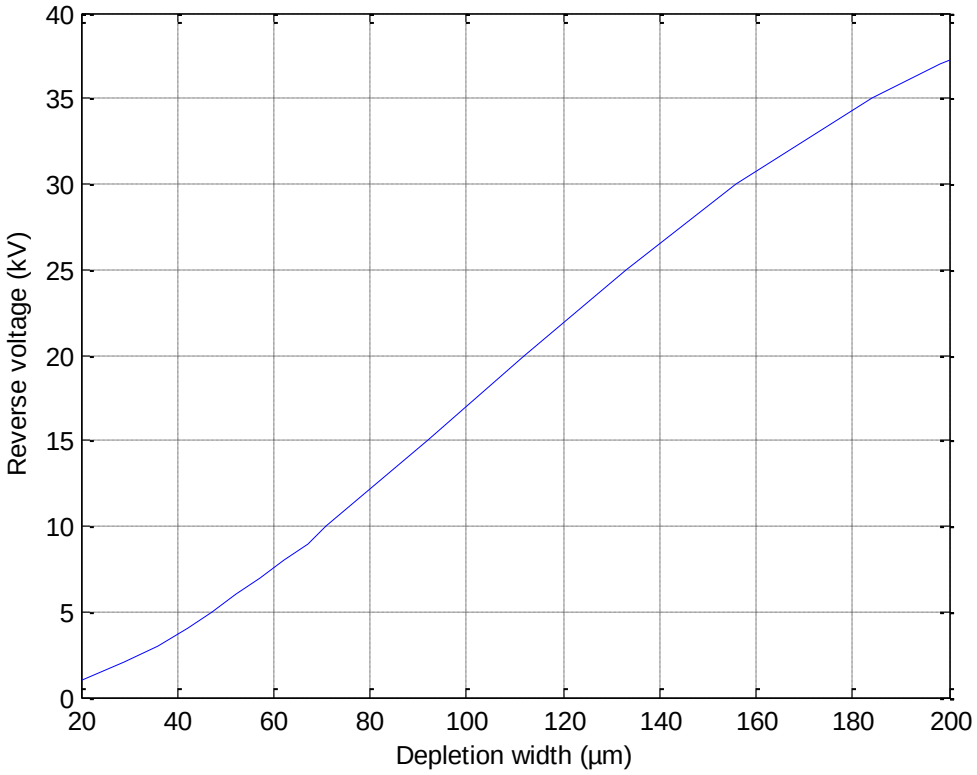


Figure 4.1 Variation of reverse voltage with depletion width for profile 1

Table 4.2 Results of depletion width and reverse voltage for profile 2 (Figure 3.2). $N_0=10^{16}\,cm^{-3}$, $m=80x10^{-4}$ cm

| Reverse Voltage (kV) | Depletion Width (µm) |
|---|---|
| 1 | 4.57 |
| 2 | 6.48 |
| 3 | 7.96 |
| 4 | 9.22 |
| 5 | 10 |
| 6 | 11 |
| 7 | 12 |
| 8 | 13 |

| | |
|---|---|
| 9 | 14 |
| 10 | 15 |
| 15 | 18 |
| 20 | 21 |
| 25 | 24 |
| 30 | 26 |
| 40 | 30 |
| 100 | 50 |
| 200 | 75 |
| 300 | 96 |
| 400 | 116 |
| 500 | 136 |
| 600 | 157 |
| 700 | 179 |
| 789 | 200 |

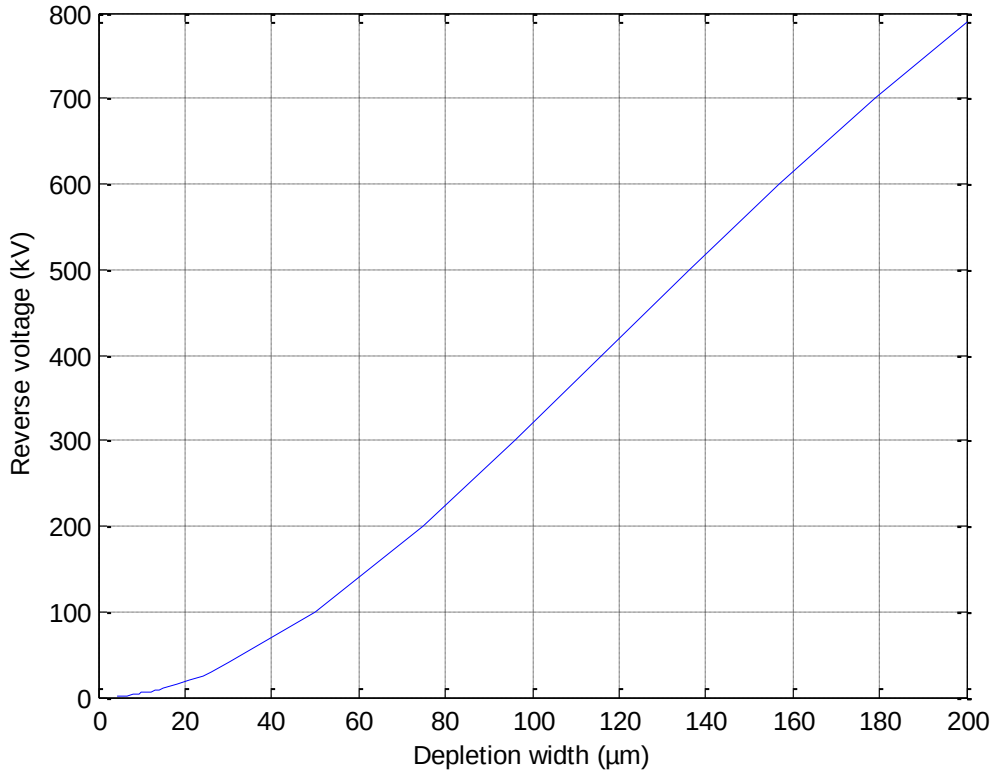


Figure 4.2 Variation of reverse voltage with depletion width for profile 2

Table 4.3 Results of depletion width and reverse voltage for profile 3 (Figure 3.3).
$N_0=10^{17}$ $cm^{-3}$, $m=70x10^{-4}$ cm

| Reverse Voltage (kV) | Depletion Width (μm) |
|---|---|
| 10 | 4 |
| 15 | 4.8 |
| 50 | 8.8 |
| 100 | 13 |
| 200 | 18 |
| 300 | 22 |
| 400 | 26 |
| 500 | 29 |
| 600 | 32 |
| 700 | 35 |
| 800 | 37 |
| 900 | 40 |
| 1000 | 42 |
| 2000 | 62 |
| 3000 | 78 |
| 4000 | 94 |
| 5000 | 108 |
| 6000 | 122 |
| 7000 | 135 |
| 8000 | 149 |
| 9000 | 163 |
| 10000 | 178 |
| 11440 | 200 |

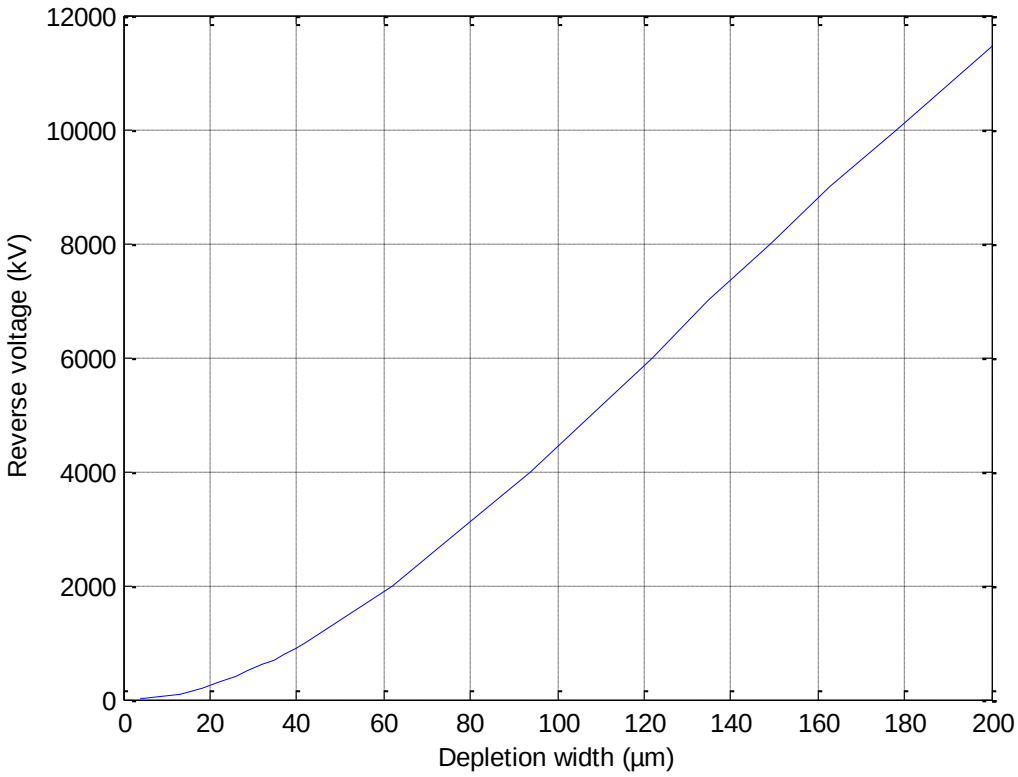


Figure 4.3 Variation of reverse voltage with depletion width for profile 3

Table 4.4 Results of depletion width and reverse voltage for profile 4 (Figure 3.4).
$N_0=10^{18}$ $cm^{-3}$, $m=60x10^{-4}$ cm

| Reverse Voltage (kV) | Depletion Width (µm) |
|---|---|
| 10 | 1.1 |
| 15 | 1.3 |
| 20 | 1.46 |
| 50 | 2.32 |
| 70 | 2.74 |
| 100 | 3.3 |
| 500 | 7.4 |
| 1000 | 11 |
| 2000 | 15 |
| 5000 | 24 |
| 10,000 | 35 |

| | |
|---|---|
| 20,000 | 51 |
| 50,000 | 86 |
| 80,000 | 115 |
| 1,00,000 | 134 |
| 1,10,000 | 143 |
| 1,20,000 | 153 |
| 1,30,000 | 162 |
| 1,40,000 | 171 |
| 1,50,000 | 181 |
| 1,69,000 | 200 |

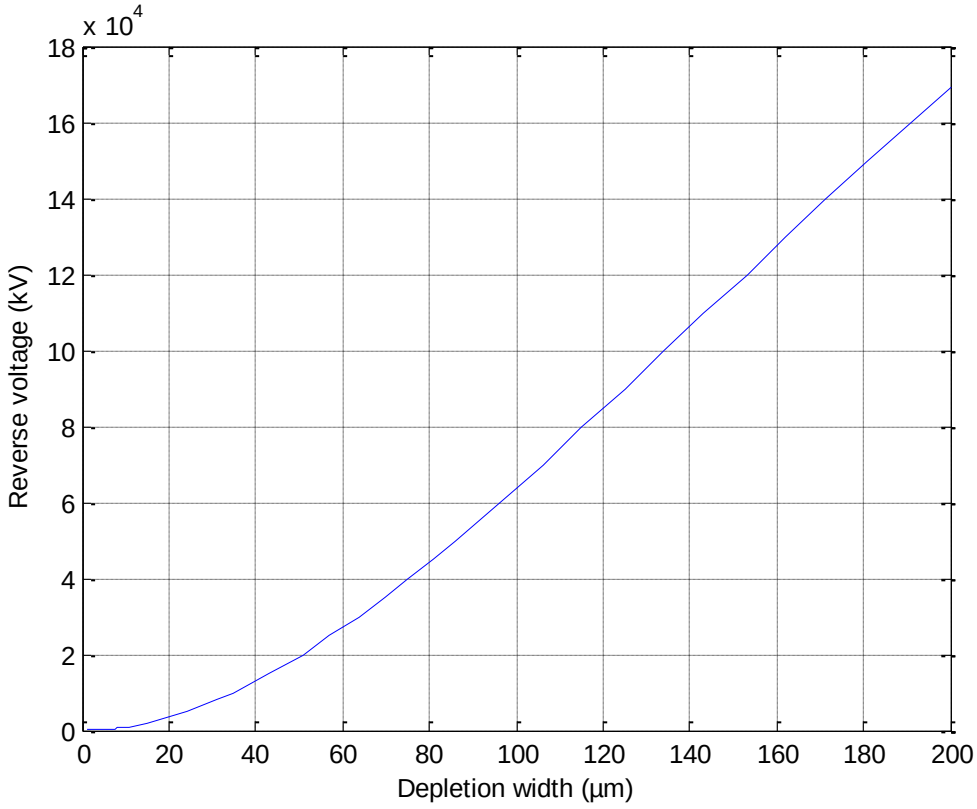


Figure 4.4 Variation of reverse voltage with depletion width for profile 4

For different values of constant m, breakdown voltage has been calculated for different values of the peak carrier concentration $N_0$.

Table 4.5 Results of breakdown voltage and peak concentration for m=50x10$^{-4}$cm

| Peak Concentration $N_0$ (cm$^{-3}$) | Breakdown Voltage $V_B$ (kV) |
|---|---|
| $10^{15}$ | 260.4 |
| $10^{16}$ | 2604 |
| $10^{17}$ | 26040 |
| $10^{18}$ | 260400 |

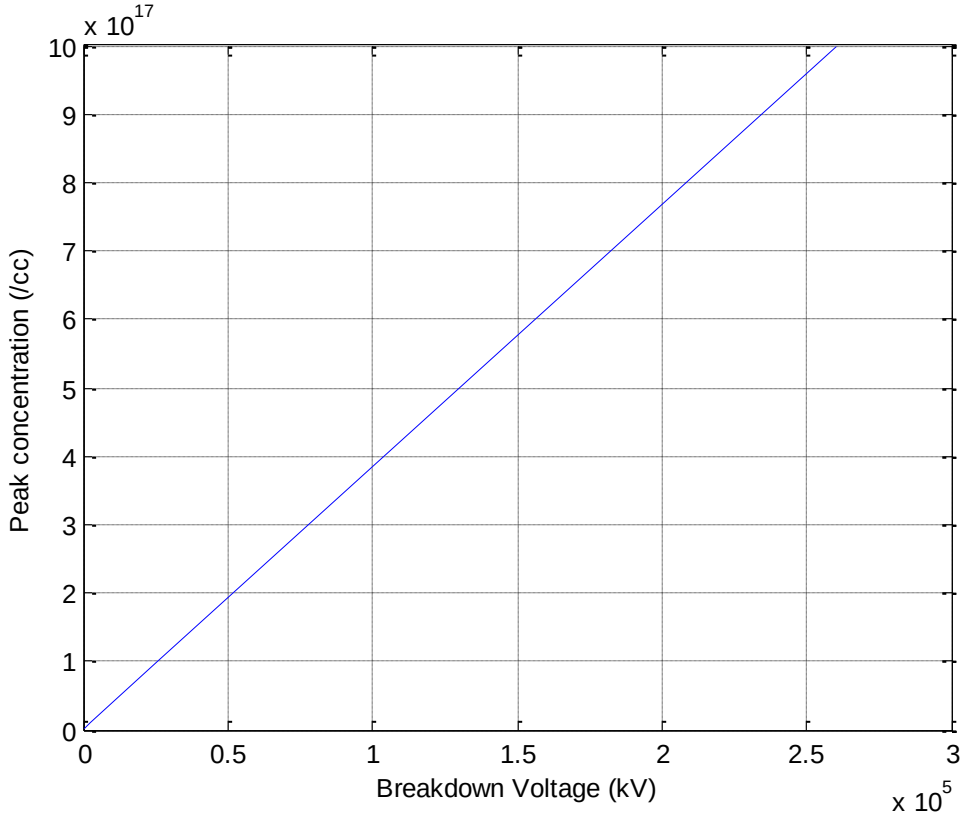


Figure 4.5 Variation of breakdown voltage with peak concentration for m=50x10$^{-4}$ cm

Table 4.6 Results of breakdown voltage and peak concentration for m=100x10$^{-4}$cm

| Peak Concentration $N_0$ (cm$^{-3}$) | Breakdown Voltage $V_B$ (kV) |
|---|---|
| $10^{15}$ | 37.2 |
| $10^{16}$ | 372 |
| $10^{17}$ | 3720 |
| $10^{18}$ | 37200 |

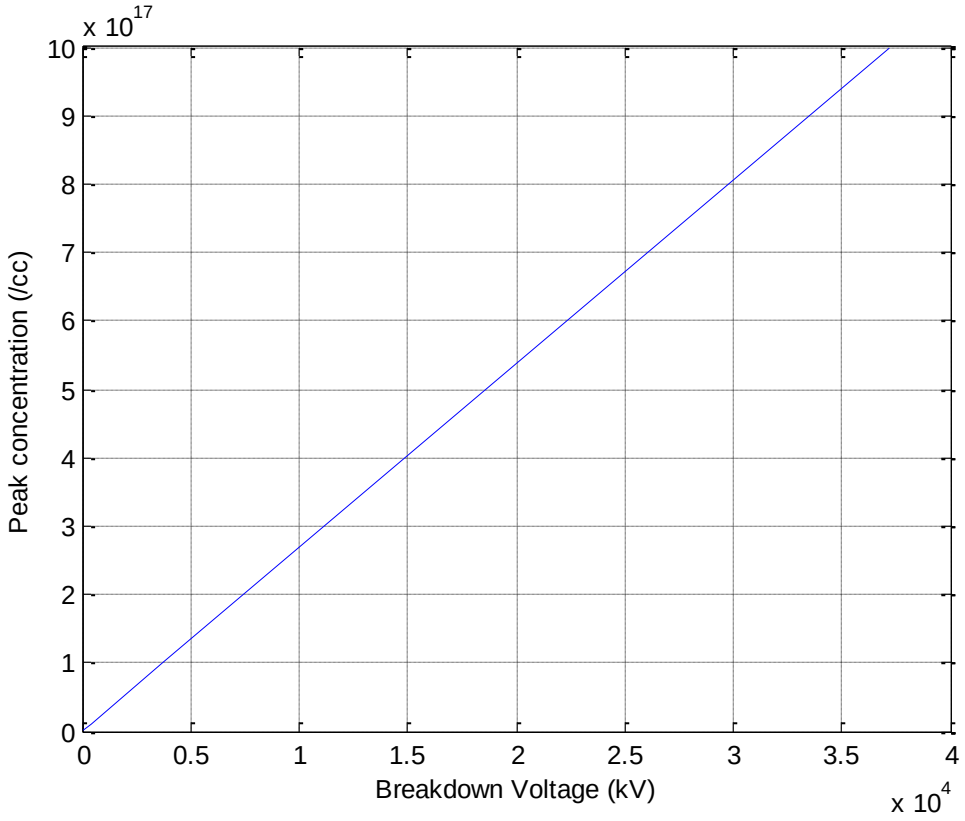


Figure 4.6 Variation of breakdown voltage with peak concentration for m=100x10$^{-4}$ cm

Table 4.7 Results of breakdown voltage and peak concentration for m=141x10$^{-4}$cm

| Peak Concentration $N_0$ (cm$^{-3}$) | Breakdown Voltage $V_B$ (kV) |
|---|---|
| $10^{15}$ | 0.22266 |
| $10^{16}$ | 2.2266 |
| $10^{17}$ | 22.266 |
| $10^{18}$ | 222.66 |

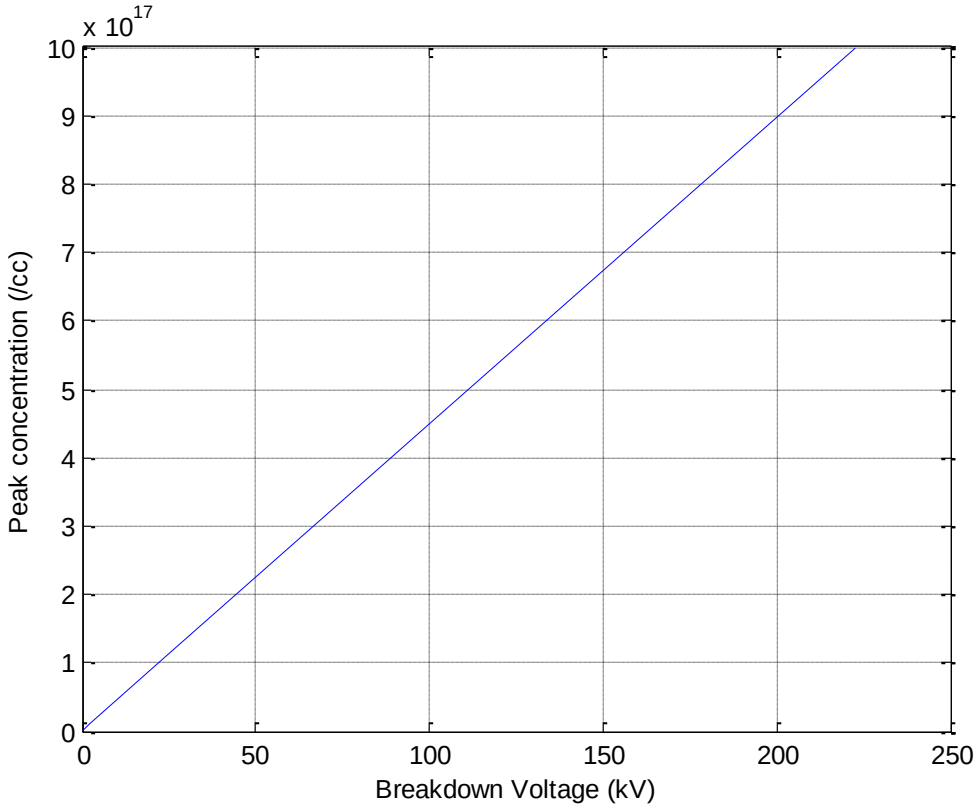


Figure 4.7 Variation of breakdown voltage with peak concentration for m=141x10$^{-4}$ cm

Table 4.8 Results of breakdown voltage and peak concentration for m=141.4x10$^{-4}$cm

| Peak Concentration $N_0$ (cm$^{-3}$) | Breakdown Voltage $V_B$ (kV) |
|---|---|
| $10^{15}$ | 0.011238 |
| $10^{16}$ | 0.11238 |
| $10^{17}$ | 1.1238 |
| $10^{18}$ | 11.238 |

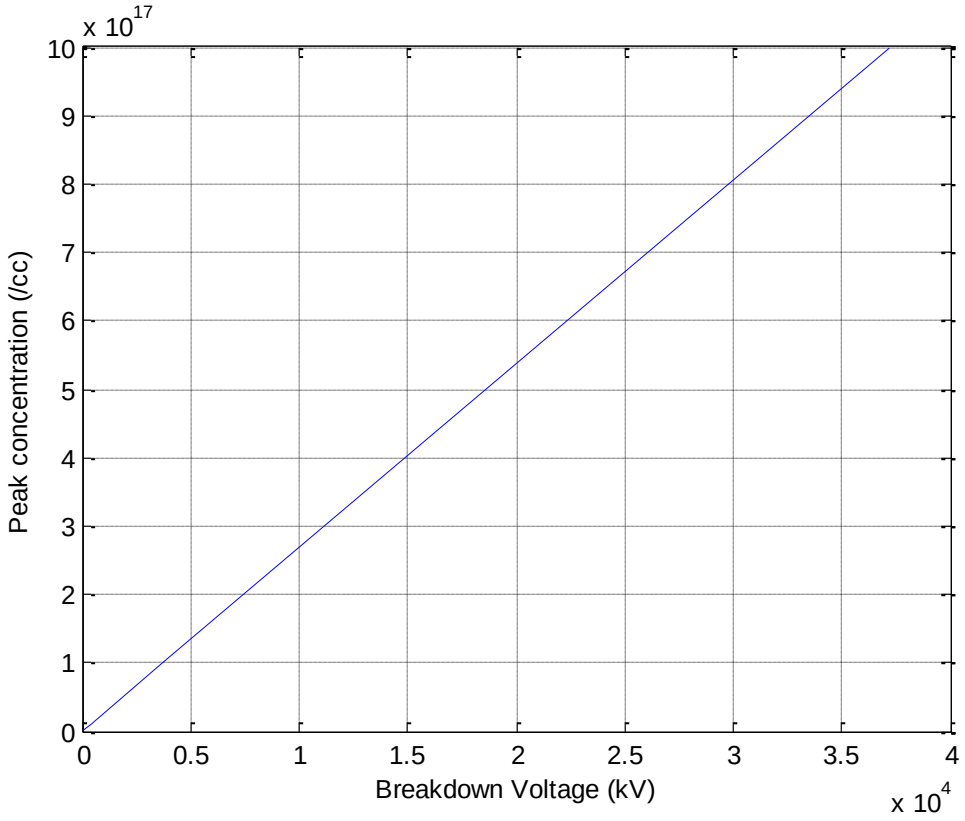


Figure 4.8 Variation of breakdown voltage with peak concentration for m=141.4x10$^{-4}$ cm

Table 4.9 Results of breakdown voltage and peak concentration for m=150x10$^{-4}$cm

| Peak Concentration $N_0$ (cm$^{-3}$) | Breakdown Voltage $V_B$(kV) |
|---|---|
| $10^{15}$ | -4.133 |
| $10^{16}$ | -41.33 |
| $10^{17}$ | -413.3 |
| $10^{18}$ | -4133 |

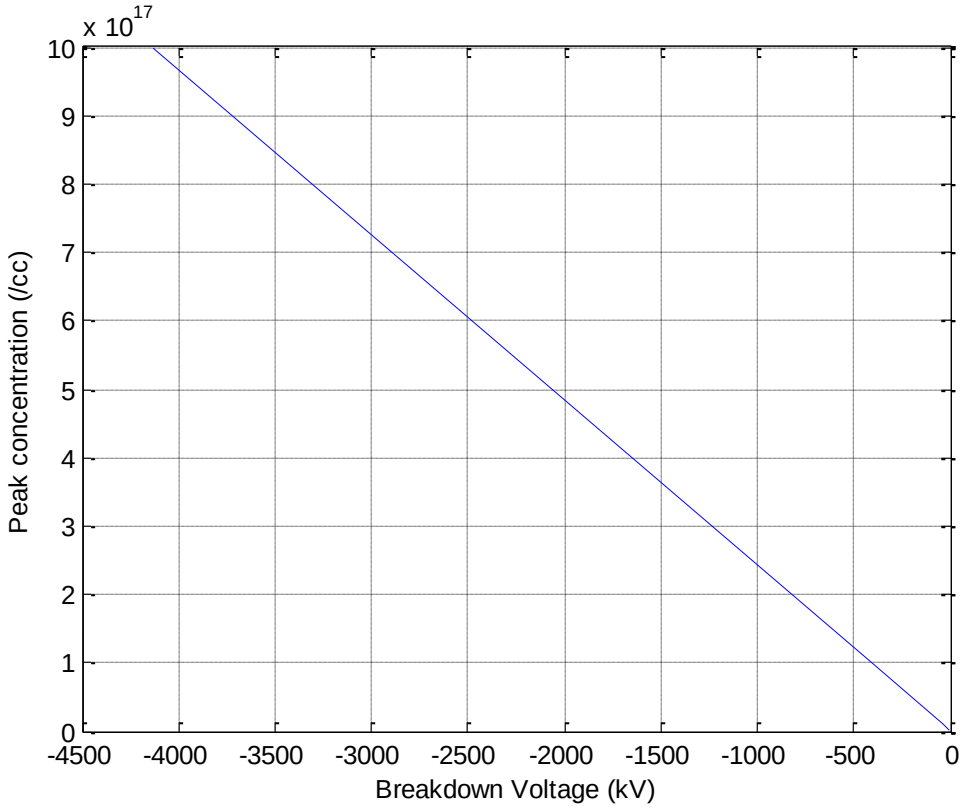


Figure 4.9 Variation of breakdown voltage with peak concentration for m=150x$10^{-4}$ cm

Now, the variation of derivative of breakdown voltage w.r.t. peak concentration is studied with respect to the values of constant m and variation of derivative of depletion width w.r.t. breakdown voltage with peak concentration. Table 4.10 and 4.11 shows the calculated values of the derivatives.

Table 4.10 Results of gradient of depletion width with breakdown voltage with respect to peak concentration

| Peak concentration $N_0$ ($cm^{-3}$) | dW/dV (µm/kV) |
|---|---|
| $10^{15}$ | 4 |
| $10^{16}$ | 0.21 |
| $10^{17}$ | 0.014667 |
| $10^{18}$ | 0.0010667 |

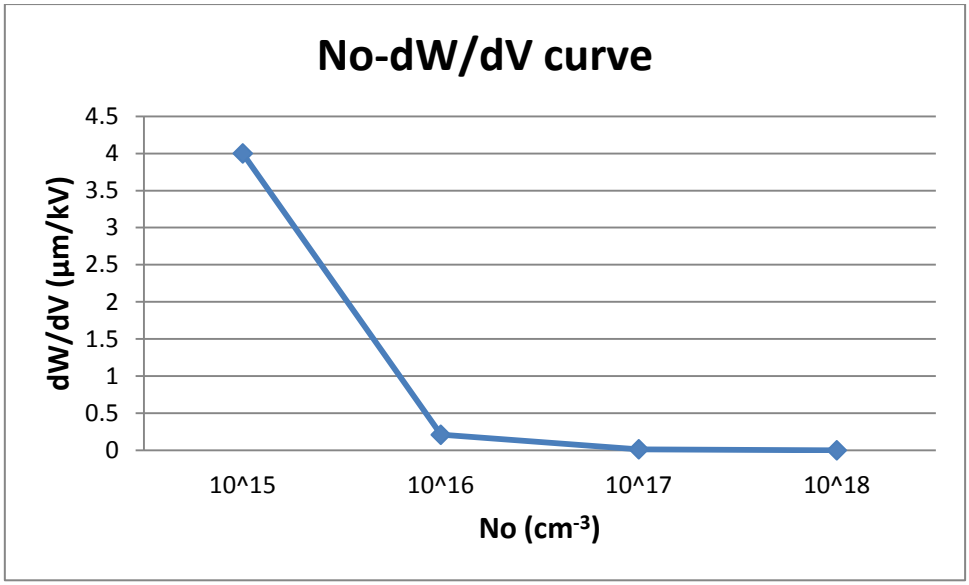


Figure 4.10 Variation of gradient of depletion width with breakdown voltage with respect to peak concentration.

Table 4.11 Results of gradient of breakdown voltage with peak concentration with respect to constant m.

| m (cm) | $dV_B/dN_0$ ($Vcm^3$) |
|---|---|
| $50x10^{-4}$ | $2.604x10^{-10}$ |
| $100x10^{-4}$ | $3.72x10^{-11}$ |
| $141x10^{-4}$ | $2.227x10^{-13}$ |
| $141.4x10^{-4}$ | $1.124x10^{-14}$ |

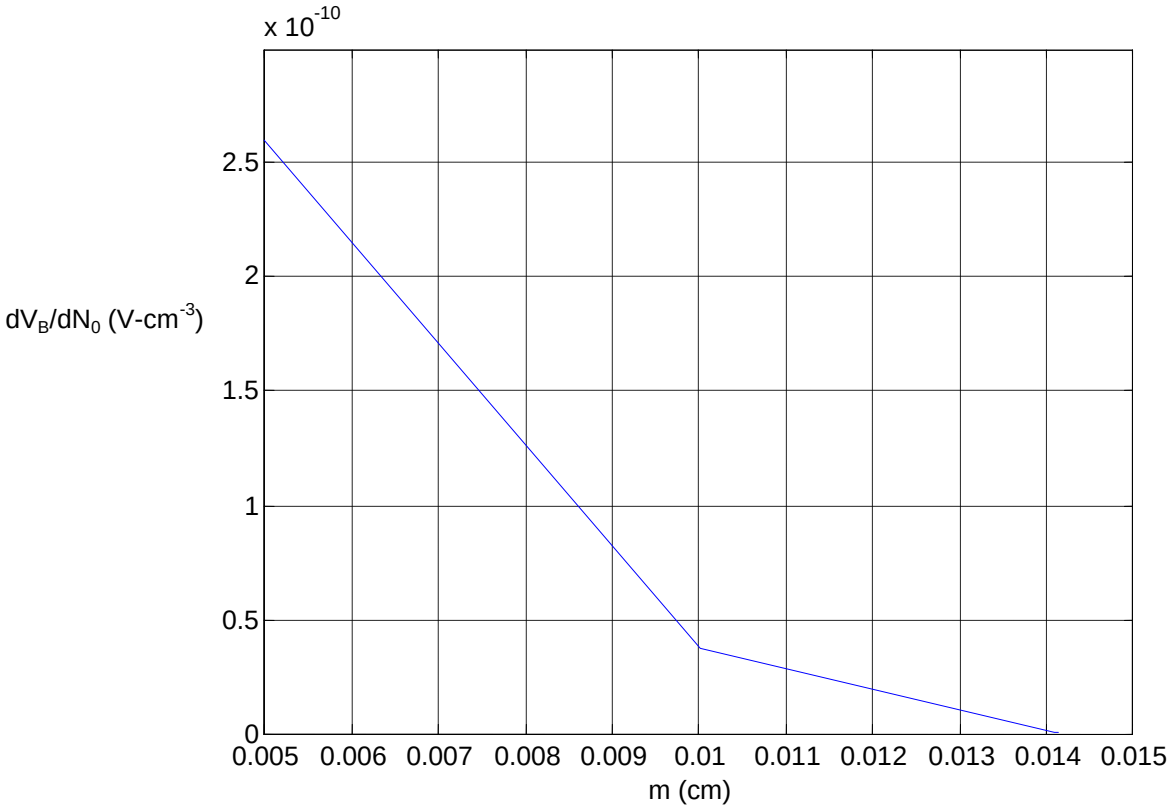


Figure 4.11 Variation of gradient of breakdown voltage with peak concentration with respect to constant m.

# CHAPTER 5

## DISCUSSION OF RESULTS OBTAINED

Various profiles that have been drawn for different values of $N_0$ and m have been shown in figures 3.1-3.4; the corresponding variations of punch through breakdown voltage with depletion region width have been shown in figures 4.1-4.4. So, it can be seen that an increase in $N_0$ with a decrease in m results in constant gradients of N(x) against x. This can be seen for values of $N_0$ of $10^{15}$ $cm^{-3}$ with m=100x$10^{-4}$ cm to $N_0$=$10^{18}$ $cm^{-3}$ with m=60x$10^{-4}$ cm.

The variation in breakdown voltage against depletion region width for 3C-SiC Schottky Barrier Diode is shown in figures 4.1-4.4. An analysis of these figures shows that the magnitude of gradient of depletion region width with breakdown voltage is found to decrease for the Gaussian profiles considered in this study. This is shown in figure 4.10. So, this means that breakdown voltage increases with an increase in depletion region width. Hence, it means that with an increase in $N_0$ associated with decrease in m gives rise to an increase in breakdown voltage with an increase in depletion region width. So, all the profiles considered here have a maximum value of depletion region width of 200µm. Hence, this study is primarily for 3C-SiC Schottky Barrier diode with a maximum device height of h=$W_{max}$=200µm.

The sequence of plots of $N_0$ against $V_B$ for 200µm thick device of 3C-SiC Schottky Barrier Diode for increasing values of m ranging from m=50x$10^{-4}$cm to 150x$10^{-4}$cm are shown in figure 4.5-4.9. An analysis of these curves shown in figure 4.11 shows that at over a range of values of $N_0$, if we consider the variation of breakdown voltage, it is seen that the variation of breakdown voltage with $N_0$ is found to increase with decreasing value of m.

In the end, we might conclude that 3C-SiC Schottky Barrier Diodes with Gaussian profiles can be used to fabricate Schottky barrier diode with thinner wafers, higher punch through breakdown voltages using higher values of $N_0$ and lower values of m.

# CHAPTER 6

# CONCLUSION AND FUTURE WORK

The present study which has been used to analyse punch through breakdown voltage of 3C-SiC Schottky Barrier Diode have been done based on using Gaussian profiles in semiconductor region of these devices. The profiles have value $N_0$ near base decreasing to lower values near Schottky contact. This was done to provide lower doping levels near contact in which wider depletion region width for higher breakdown voltage can be accommodated. The higher doping levels approaching $N_0$ at base in lower part of device gives rise to low parasitic series resistance which reduce substantially power dissipation of the device.

The results of the analysis have already been discussed in chapter 5 where it was already been established that increasing value of $N_0$ and decreasing m gives rise to higher breakdown voltages. Finally, the last portion analysis given in chapter 5 points to the fact that an increase in $N_0$ with a decrease in m gives rise to an increase in breakdown voltage with increasing depletion region width. Lastly, it has been shown in chapter 5 that a decrease in m can provide an increase in breakdown voltage with decreasing $N_0$.

This type of analysis can be used for designing devices which have higher breakdown voltage, lower device height and smaller depletion region width by using other profiles especially widely used complementary error function (erfc) profile. It remains to be seen whether some non-linear profile like hyper abrupt junction profile can yield still higher breakdown voltage than those which have been estimated in this work using Gaussian profile.

## REFENCES

[1] K. Jarrendahl and Robert F. Davis, "Materials Properties and Characterization of SiC, Semiconductors and Semimetals", SiC Materials and Devices, Vol. 52, pp. 1-20, 1998.

[2] G. R. Fisher and P. Barnes, "Towards a Unified View of Polytypism in Silicon Carbide‖, Philosophical Magazine", Vol. 61, pp. 217-236, 1990.

[3] O. Kordina, "Growth and Characterisation of Silicon Carbide Power Device Material", Ph.D. thesis, Lonkoping University, 1994.

[4] H-E. Nilsson, M. Hjelm, C. Frojdh, C. Persson, U. Sannemo and C. S. Petersson, "Full Band Monte Carlo simulation of electron transport in 6H-SiC", Journal of Applied Physics, Vol. 86, pp. 965-973, 1999.

[5] W.J. Schaffer, G.H. Negley, K.G. Irvine and J.W. Palmour, "Conductivity Ansisotropy in Epitaxial 6H and 4H SiC", MRS Proceedings, Vol. 339, pp. 595-600, 1994.

[6] I.A. Khan and J.A. Cooper, "Measurement of High-Field Electron Transport in Silicon Carbide", IEEE Transactions on Electron Devices, Vol. 47, pp. 269-273, 2000.

[7] H-E. Nilsson, U. Sannemo, and C.S. Petersson , "Monte Carlo simulation of electron transport in 4H–SiC using a two band model with multiple minima", Journal of Applied Physics, Vol. 80, pp. 3365-3369, 1999.

[8] Kent Bertilsson, "Simulation and Optimization of SiC Field Effect Transistors", Doctoral Thesis , KTH Microelectronics and Information Technology, Stockholm, Sweden 2004.

[9] M. Dudley, W. Huang, W.M. Vetter, P.G. Neudeck, J.A. powell, "Synchrotron White Beam Topography Studies of 2H SiC Crystals", Materials Science Forum, Vol. 338-342, pp. 465-468, 2000.

[10] H-E. Nilsson and M. Hjelm, "Monte Carlo simulation of electron transport in 2H-SiC using a three valley analytical conduction band model", Journal of Applied Physics, Vol. 86, pp. 6230-6233, 1999.

[11] Stephen E. Saddow, Anant Agarwal, "Advances in Silicon Carbide Processing and Applications", first edition, Artech House, Inc. Boston, London 2004, www.artechhouse.com

[12] Hudgins, "Wide and Narrow Bandgap Semiconductors for Power Electronics: A New Valuation",Journal of Electronic Materials, Vol. 32, No. 6, pp. 471- 477,2003.

[13] M. Roschke, F. Schwiertz, "Electron mobility Models for 4H, 6H, and 3C SiC", IEEE trans. Elec. Dev. Vol. 48, No. 7, pp.1442-1447, 2001.

[14] J.Spits, M.R.Melloch, J.A.Cooper, Jr. And M.A.Capano, "High-Voltage (2.6kV) Lateral DMOSFETs in 4H-SiC", IEEE Electron Device Lett., 19,100(1998).

[15] Virgil B. Shields, "Applications of Silicon Carbide for High Temperature Electronics and Sensors", California Institute of Technology.

[16] Fuster, Marco A., "Skateboard grip tape", U.S. Patent 5,622,759, 1997.

[17] unipass.com, "Ceramics for turbine engines", Retrieved 2009-06-06.

[18] topmost10.com, "Top 10 Fast Cars", Archived from the original on 2009-03-26. Retrieved 2009-06-06.

[19] Bayliss, Colin R., "Transmission and distribution electrical engineering", Newnes, pp. 250, ISBN 0-7506-4059-6, 1999.

[20] Stringfellow, Gerald B., "High brightness light emitting diodes", Academic Press, pp. 48, 57, 425, ISBN 0-12-752156-9, 1997.

[21] Petrovsky, Gury T., Tolstoy, Michael N., Lubarsky, Sergey V., Khimitch, Yuri P., Robb, Paul N., Tolstoy; Lubarsky; Khimitch, Robb, "2.7-meter-diameter silicon carbide primary mirror for the SOFIA telescope", In Stepp, Larry M. Proc. SPIE, Advanced Technology Optical Telescopes Vol. 2199: 263, 1994.

[22] Munish Vashishath and Ashoke K. Chatterjee, "Recent trends in silicon carbide device research", Mj. Int. J. Sci. Tech., 2(03), pp. 444-470, 2008.

[23] L.Yuan, M.R.Melloch, J.A.Cooper and K.J.Webb, "Silicon Carbide IMPATT Oscillators for High-Power Microwave and Millimeter-Wave Generation", IEEE Cornell Conference on Advanced Concepts in High Speed Semiconductor Device

[24] L.Yuan, M.R.Melloch, J.A.Cooper and K.J.Webb, "Silicon Carbide IMPATT Oscillators for High-Power Microwave and Millimeter-Wave Generation", IEEE Cornell Conference on Advanced Concepts in High Speed Semiconductor Devices and Circuits, Ithaca,NY, pp.158-167,Aug-2000.

[25] W.Xie, J.A.Cooper, M.R.Melloch, J.W.Palmour and C.H.Carter, Jr., "A Vertically Integrated Bipolar Storage Cell in 6H Silicon Carbide for Nonvolatile Memory Applications" IEEE ,Vol. 15, pp. 212-214, 1994.

[26] S. Sridevan, P. K. Mclarty, and B. J. Baliga, "On the presence of aluminum in thermally grown oxides on 6H-silicon carbide power MOSFETs", IEEE Electron Device Lett., Vol. 17, pp. 136-138,1996.

[27] Mietek Bakowski, Adolf Schöner, Per Ericsson, Helena Strömberg, Hiroyuki Nagasawa,and Masayuki Abe, "Development of 3C-SiC MOSFETs", Journal of Telecommunication and information Technology,2/2007.

[28] Stephen E. Saddow, Anant Agarwal, “Advances in Silicon Carbide Processing and Applications”, first edition, Artech House, Inc. Boston, London, 2004.

[29] N.F. Mott, ―Note on the Contact between a Metal and an Insulator or Semiconductor‖, Mathematical Proceedings of the Cambridge Philosophical Society, Vol. 34, pp. 568-572, 1938.

[30] B. J. Baliga, “Silicon Carbide power devices”, World Scientific publication, Singapore, 2005.

[31] A. J. Steckl and J. N. Su, ”High Voltage Temperature-Hard 3C-SiC Schottky Diodes Using All-Ni Metallization”, IEEE Trans. Electronics Device, pp 695-698, 1993.

[32] Praveen Shenoy, Akira Moki, B.J.Baliga, Dev Alok, K.Wongchotigul and M.Spencer, ” Vertical Schottky Barrier Diodes on 3C-Sic Grown on Si”, IEEE Trans. Electronics Device, pp. 411-414, 1994.

[33] R. Raghunathan, D. Alok, and B. J. Baliga―High Performance of High- Voltage 4H-SiC Schottky Barrier Diodes‖, IEEE Electron Device Letters, Vol. 16, pp. 280-282, 1995.

[34] Carl-Mikael Zetterling, Fanny Dahlquist, Nils Lundberg, Mikael oè stling, Kurt Rottner and Lennart Ramberg, “Junction Barrier Schottky diodes in 6H SiC”, Solid-State Electronics Vol. 42, No. 9, pp. 1757±1759,1998.

[35] G. Brezeanu, M. Badila, B. Tudor, J. Millan, P. Godignon, Marie Laure Locatell, J. P. Chante, G. Amaratunga, F. Udrea, A. Mihaila, ” Accurate modeling of Ni/6H-SiC Schottky Barrier Diodes (SBD) forward characteristics at high current densities”, IEEE Electron Device Letters, 2000.

[36] Gheorghe Brezeanu, Marian Badila, Bogdan Tudor, José Millan,Philippe Godignon, Florin Udrea, G. A. J. Amaratunga and Andrei Mihaila,” Accurate Modeling and Parameter Extraction for 6H-SiC Schottky Barrier Diodes (SBDs) With Nearly Ideal Breakdown Voltage”, IEEE Transactions on Electron Devices, Vol. 48, No.9, 2001.

[37] X. Jorda, D. Tournier, M. Vellvehi, A. Perez, R. Perez, P. Godignon, J. Millan, “Comparitive valuation of High Current SiC Schottky Diodes and Si PN Junction Diodes”, Spanish Conference on Electron Devices, pp. 87-90, 2005.

[38] J.W. Palmour, “Energy Efficient Wide Bandgap Devices”, Compound Semiconductor IC Symposium, pp. 4-7, 2006.

[39] Jens Eriksson, Ming Hung Weng, Fabrizio Roccaforte, Filippo Giannazzo, Stefano Leone,Vito Raineri, “Toward an ideal Schottky barrier on 3C-SiC”, Applied Physics Letters, Vol. 95, 2009.

[40] R. Talwar and A.K. Chatterjee, “A Method to Calculate the Voltage- Current Characteristics of 4H SiC Schottky Barrier Diode”, Maejo International Journal of Science and Technology, Vol. 3, pp. 287-294, 2009.

[41] W. Janke, A. Hapka, “The current-voltage characteristics of SiC Schottky barrier diodes with the self-heating included”, Koszalin University of Technology, Poland, 2010.

[42] Jens Eriksson, Fabrizio Roccaforte, Sergey Reshanov, Stefano Leone, Filippo Giannazzo, Raffaella LoNigro, Patrick Fiorenza, Vito Raineri, “Nanoscale characterization of electrical transport at metal/3C-SiC interfaces”, Nanoscale Research Letters, 2011.

[43] Press conference, HOYA Corporation, Mono-crystal 3C-SiC large size substrate, Japan, 2012.

[44] R.J. Michael et.al., “Innovative 3C-SiC on SiC via Direct Wafer Bonding”, Materials Science Forum, Vol. 740-742, pp. 271-274, 2013.

[45] K. Shenai, “Optimization of 4H-SiC Power Schottky Barrier Diodes”, IEEE Energytech, 2013.

[46] Shamim Ahmed, H. Alan Mantooth, Mihir Mudholkar and Ranbir Singh, “Characterization and Modeling of SiC Junction Barrier Schottky Diode for Circuit Simulation”, Control and Modeling for Power Electronics (COMPEL), 2013.

[47] Yan Liu, Chao Zhang, Zhitang Song, Bo Liu, Guanping Wu, Jia Xu, Lianhong Wang, Lei Wang, Zuoya Yang, and Songlin Feng, “Cost-Effective Schottky-Barrier Diode Array with Ni–Silicidation Accessing Low Power Phase-Change Memory”, IEEE Transactions on Electron Devices, Vol. 61, No. 3, 2014.

[48] Munish Vashishath, “Analysis and Design of Robust Power Double Implanted MOSFET on 6H silicon carbide wafers”, Doctoral Thesis, Thapar University, 2010.